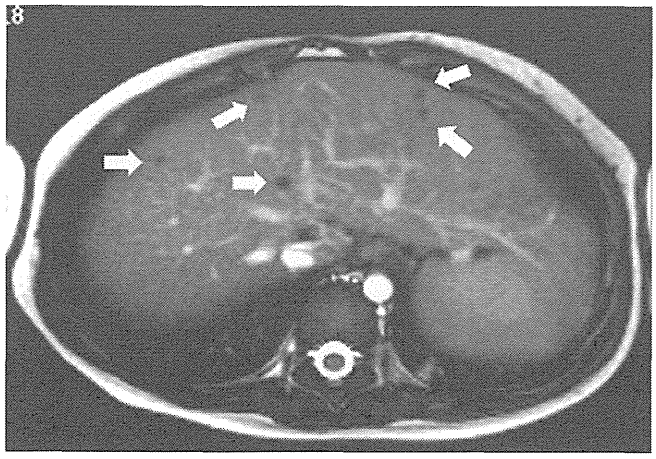

Fig. 1 Abdominal magnetic resonance image obtained at 1 year and 4 months shows multiple nodules (arrows) varying in size in the liver, which presented as a low-intensity area on T2-weighted imaging.

as low-intensity areas on T2-weighted images (see Fig. 1) and high-intensity areas on T1-weighted images without contrast enhancement. The number of nodules in his liver increased from the time of the MRI examination performed at the age of 1 year and 4 months. In addition, a transient elevation in the patient's serum ammonia levels (290 μg/dL) and impaired consciousness with the onset of fever and a poor appetite were observed at the age of 2 years. The clinical course during this episode showed positive results. Liver biopsies were performed during a laparotomy to inspect the progress of the liver cirrhosis at the age of 2 years and 1 month. He was suspected of having MRCD, which is one of the main causes of hepatic disorder, because all other differential diagnoses for hepatic cirrhosis had been ruled out. Thus, we were able to examine the mitochondrial respiratory chain function in the liver biopsy samples. Liver respiratory chain complexes I and IV were found to be deficient in this patient using both a respiratory chain enzyme assay (Table 1) and a liver blue native polyacrylamide gel electrophoresis (BN-PAGE).[3] Complex I and IV activities were below the normal level (<30%)[4] of the CS ratio. Liver BN-PAGE showed an extremely weak complex I and IV band in this patient. In addition, the rate of mtDNA and nDNA (quantitative polymerase chain reaction) was about 95.4% (normal level). Mitochondrial DNA depletion syndrome was ruled out. The macroscopic anatomy showed diffuse nodules on the surface of the liver. The microscopic findings for the liver are shown in Figure 2. Coenzyme Q, vitamin C, vitamin E, and carnitine therapy were initiated at an age of 2 years and 3 months. The patient continues to exhibit normal physical and mental development after diagnosis. His weight was 21.9 kg (+0.3SD score) and height was 117.5 cm (+0.6SD score) at the age of 6 years. However, the patient's transaminase levels were 56–311 IU/L (AST) and 31–174 IU/L (ALT), and findings of the follow-up MRI at the age of 5 years suggested progressive changes in liver cirrhosis. MRI demonstrated right lobe atrophy, enlargement of the left lobe, and an irregular edge border of the liver (Fig. 3a,b). MRI revealed a well-circumscribed mass 16 × 11-mm (see arrow) in liver segment VI (Fig. 3c). In addition to this mass, MRI demonstrated nodules 4–8 mm in size in the liver parenchyma, which were visualized as slightly hyperintense lesions on the T2-weighted images and as hypointensities on the T1-weighted images (Fig. 3c).

Table 1 Respiratory chain enzyme assay in the liver of the patient

	Complex I	Complex II	Complex III	Complex IV	CS
% of normal	14	37	62	15	54
CS ratio (%)	26	67	111	27	
Complex II ratio (%)	38		165	40	

Discussion

We reported a boy with chronic hepatic disorder and cirrhosis who was found to have mitochondrial respiratory chain complex I and IV deficiency during his infant period. In our experience, deficiencies of complexes I and IV account for about 15% of all diagnosed cases of MRCD in Japanese subjects. Nine clinical case reports of complex I and IV deficiencies, including adult subjects, were reported between 1988 and 2010. No specific manifestations of complex I and IV deficiency were observed in the past reports. The patient's blood lactate/pyruvate rate was almost normal in the clinical course. However, a normal lactate level does not exclude respiratory chain defects in MRCD, including mitochondrial hepatopathy.[5,6] The molecular and genetic causes of complex I and IV deficiency are not clear.

The histological findings of liver biopsy specimens from patients with primary mitochondrial hepatopathies reveal individual, non-specific histologic and ultrastructural findings, with predominant microvesicular steatosis and canalicular cholestasis.[7] Periportal and centrilobular fibrosis are characteristic features, and the dropout of broad bands of hepatocytes leads to micronodular cirrhosis.[7] Thus, the histologic findings of this case were highly suggestive of MRCD. In addition, if electron micrographs revealed morphological abnormality of mitochondria in liver biopsies, they would have been useful for confirming diagnosis of MRCD.

With respect to MRI findings, nodules which were found at the age of 1 year were not detected at the age of 5 years. The nodules in Figure 1 might be regenerative nodules (RN) associated with hepatic cirrhosis, because RN typically appear as hypointense lesions on T2-weighted images[8] and the imaging findings at the age of 5 years were typical of hepatic cirrhosis. Furthermore, focal nodular hyperplasia, which is one of the important differential diagnoses of hepatic nodules in infants, was excluded on the basis of the high signal intensity in the non-enhanced T2-weighted images.[9] However, these nodules were so small that they were difficult to evaluate by MRI or histopathology.

Findings of progressive liver cirrhosis changes were observed in a liver MRI at the age of 5 years (Fig. 3a–c). The 16 × 11-mm mass in Figure 3c (see arrow) was visualized as a hyperintensity on opposed-phase T1-weighted gradient-echo images and as a slightly low-intensity area on the T2-weighted images. Focal

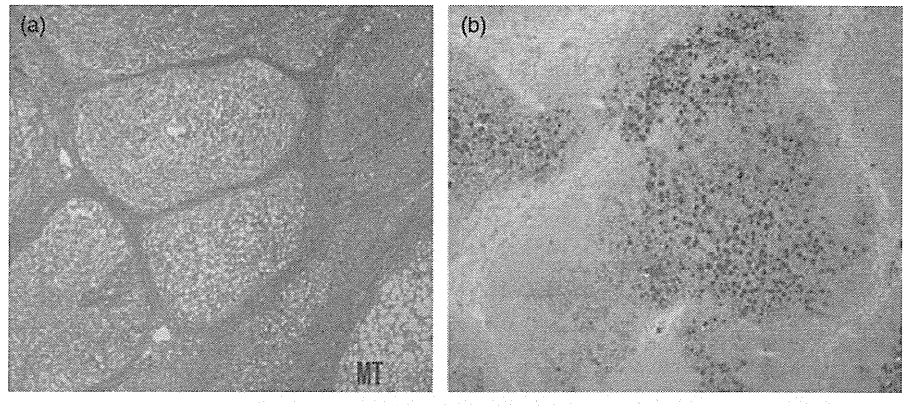

Fig. 2 (a) Masson trichrome stain: Microscopic findings in the liver show the division of a hepatic lobule into nodules by bridging fibrosis in the liver tissue. (b) Sudan III stain: Liver tissues show heterogeneous hepatic steatosis in each septum. Portal fibrosis was observed in liver tissues without inflammation (not shown).

nodular hyperplasia was excluded because the mass did not show the high-intensity on the non-enhanced T2-weighted images. The size remained unchanged as compared to the previous year. Thus, the mass was suspected to be a regenerative nodule or adenomatous hyperplasia, associated with hepatic cirrhosis. In addition to this mass, MRI in Figure 3c demonstrated nodules 4–8 mm in size in the liver parenchyma. Although these nodules were found to contain lipids inside, as they were visualized as low-intensity areas on opposed-phase T1-weighted gradient-echo images and as high-intensity areas on in-phase images, they were too small to evaluate in detail.

The early and accurate diagnosis of MRCD is important because appropriate therapy and guidance can be provided to the patient and his/her family before the condition worsens. MRCD is difficult to diagnose because the clinical manifestations do not depend on the type of complex deficiency. Some previous patients have died of hepatic failure during the neonatal period or infancy, while other patients never develop hepatic disease despite long-term follow-up observation.[1] However, it is conceivable that a regular screening for secondary liver cancer is necessary for the patient with progressive cirrhosis, along with MRCD during his infant period.[10]

With respect to diagnosis, regular ultrasound or CT examinations are needed for infants with idiopathic chronic hepatitis because multiple nodules in the liver gradually appeared in the patient. Furthermore, we conclude that an examination of the mitochondrial respiratory chain function should be performed along with a liver biopsy if MRCD is suspected as a possible differential diagnosis of idiopathic hepatitis under the signs of liver cirrhosis, as in this case.

Acknowledgments

The authors report no conflicts of interest. We have no disclosures to make and have not received any financial support.

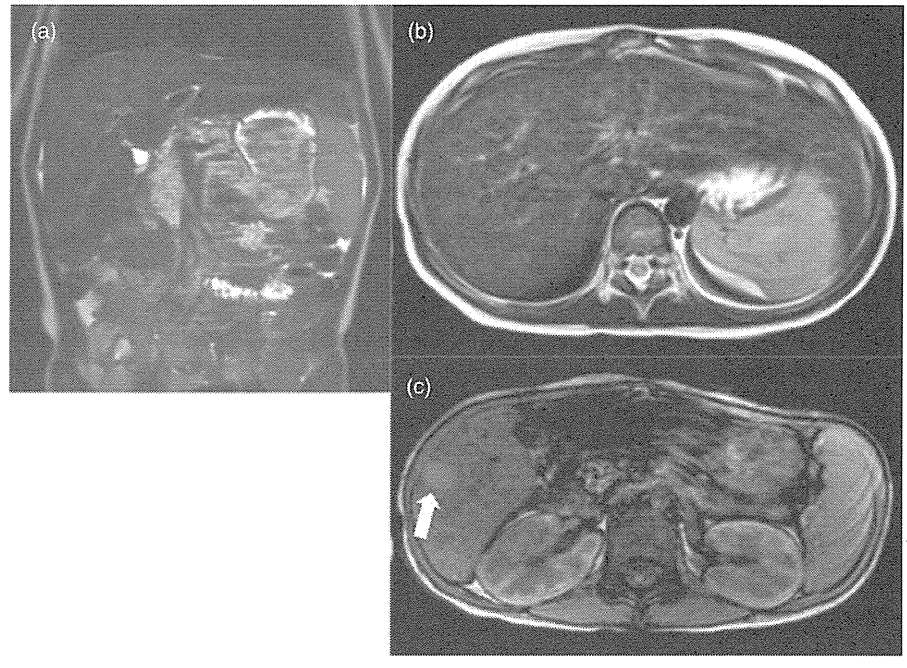

Fig. 3 (a) T2-weighted magnetic resonance image (MRI) demonstrates right lobe atrophy, enlargement of the left lobe, and an irregular edge border of the liver at the age of 5 years. (b) T2-weighted MRI shows marked hyperintensity in the periportal region. The hepatic parenchyma appears heterogeneously enhanced in the delayed phase. (c) T1-weighted MRI revealing a well-circumscribed 16 × 11-mm mass (see arrow) in liver segment VI. This mass is visualized as a hyperintensity on opposed-phase T1-weighted gradient-echo images and as a slightly lower-intensity area on the T2-weighted images. In addition to this mass, MRI demonstrates nodules 4–8 mm in size in the liver parenchyma, which are visualized as slightly hyperintense lesions on the T2-weighted images and as hypointensities on the T1-weighted images.

References

1 Carcia-cazorla A, De Lonlay P, Rustin P *et al.* Mitochondrial respiratory chain deficiencies expressing the enzymatic deficiency in the hepatic tissue: a study of 31 patients. *J. Pediatr.* 2006; **149**: 401–5.
2 Lee WS, Sokol RJ. Mitochondrial hepatopathies: advances in genetics and pathogenesis. *Hepatology* 2007; **45**: 1555–65.
3 Schagger H, Aquila H, von Jagow G. Coomassie blue-sodium dodecyl sulfate- polyacrylamide gel electrophoresis for direct visualization of polypeptides during electrophoresis. *Anal. Biochem.* 1988; **173**: 201–55.
4 Bernier FP, Boneh A, Dennett X, Chow CW, Cleary MA, Thorburn DR. Diagnostic criteria for respiratory chain disorders in adults and children. *Neurology* 2002; **59**: 1406–11.
5 Kirby MD, Crawford M, Cleary MA, Dahl HH, Dennet X, Thorburn DR. Respiratory chain complex I deficiency: an underdiagnosed energy generation disorder. *Neurology* 1999; **52**: 1255–64.
6 Fellman V, Kotarsky H. Mitochondrial hepatopathies in the newborn period. *Semin. Fetal Neonatal Med.* 2011; **16**: 222–8.
7 Suchy FJ, Sokol RJ, Balistreri WF. *Liver Disease in Children*, 3rd edn. Cambridge University Press, Cambridge, 2007; 803–29.
8 Hussain SM, Terkivatan T, Zondervan PE *et al.* Focal nodular hyperplasia: Findings at state-of-the-art MR imaging, US, CT, and pathologic analysis. *Radiographics* 2004; **24**: 3–17.
9 Hanna RF, Aguirre DA, Kased N, Emery SC, Peterson MR, Sirlin CB. Cirrhosis-associated hepatocellular nodules: correlation of histopathologic and MR imaging features. *Radiographics* 2008; **28**: 747–69.
10 Scheers I, Bachy V, Stephenne X, Sokal EM. Risk of hepatocellular carcinoma in liver mitochondrial respiratory chain disorders. *J. Pediatr.* 2005; **146**: 414–7.

Anal Bioanal Chem (2013) 405:1345–1351
DOI 10.1007/s00216-012-6532-3

ORIGINAL PAPER

Intracellular in vitro probe acylcarnitine assay for identifying deficiencies of carnitine transporter and carnitine palmitoyltransferase-1

Jamiyan Purevsuren · Hironori Kobayashi · Yuki Hasegawa · Kenji Yamada · Tomoo Takahashi · Masaki Takayanagi · Toshiyuki Fukao · Seiji Fukuda · Seiji Yamaguchi

Received: 24 July 2012 / Revised: 10 October 2012 / Accepted: 30 October 2012 / Published online: 10 November 2012

Abstract Mitochondrial fatty acid oxidation (FAO) disorders are caused by defects in one of the FAO enzymes that regulates cellular uptake of fatty acids and free carnitine. An in vitro probe acylcarnitine (IVP) assay using cultured cells and tandem mass spectrometry is a tool to diagnose enzyme defects linked to most FAO disorders. Extracellular acylcarnitine (AC) profiling detects carnitine palmitoyltransferase-2, carnitine acylcarnitine translocase, and other FAO deficiencies. However, the diagnosis of primary carnitine deficiency (PCD) or carnitine palmitoyltransferase-1 (CPT1) deficiency using the conventional IVP assay has been hampered by the presence of a large amount of free carnitine (C0), a key molecule deregulated by these deficiencies. In the present study, we developed a novel IVP assay for the diagnosis of PCD and CPT1 deficiency by analyzing intracellular ACs. When exogenous C0 was reduced, intracellular C0 and total AC in these deficiencies showed specific profiles clearly distinguishable from other FAO disorders and control cells. Also, the ratio of intracellular to extracellular C0 levels showed a significant difference in cells with these deficiencies compared with control. Hence, intracellular AC profiling using the IVP assay under reduced C0 conditions is a useful method for diagnosing PCD or CPT1 deficiency.

Keywords Fatty acid oxidation · Carnitine cycle disorder · Acylcarnitine profile · ESI-MS/MS

J. Purevsuren · H. Kobayashi · Y. Hasegawa · K. Yamada · T. Takahashi · S. Fukuda · S. Yamaguchi (✉)
Department of Pediatrics, Shimane University School of Medicine, 89-1 Enya,
Izumo, Shimane 693-8501, Japan
e-mail: seijiyam@med.shimane-u.ac.jp

M. Takayanagi
Division of Metabolism, Chiba Children's Hospital,
Chiba 266-0007, Japan

T. Fukao
Department of Pediatrics, Graduate School of Medicine,
Gifu University,
Gifu, Gifu 501-1194, Japan

T. Fukao
Medical Information Sciences Division, United Graduate School of Drug Discovery and Medical Information Sciences,
Gifu University,
Gifu, Gifu 501-1194, Japan

J. Purevsuren
Medical Genetics Laboratory,
National Center for Maternal and Child Health,
Khuvisgalchdyn street, Bayangol district,
Ulaanbaatar 210624, Mongolia

Introduction

L-Carnitine plays an essential role in the transfer and activation of long-chain fatty acids across the outer and inner mitochondrial membranes during which it is acted upon by enzymes including carnitine transporter (OCTN2), carnitine palmitoyltransferase-1 (CPT1), carnitine palmitoyltransferase-2 (CPT2), and carnitine acylcarnitine translocase (CACT) (Fig. 1) [1, 2]. Carnitine penetrates into cells across the plasma membrane against a high concentration gradient of free carnitine with the aid of the plasma membrane OCTN2 protein encoded by the SLC22A5 gene [3]. Deficiency of OCTN2 causes primary carnitine deficiency (PCD, OMIM 212140), which is characterized by systemic carnitine deficiency in tissues and blood but in concord with increased excretion of free L-carnitine in the urine [4–6]. Clinical symptoms in patients with PCD such as cardiomyopathy,

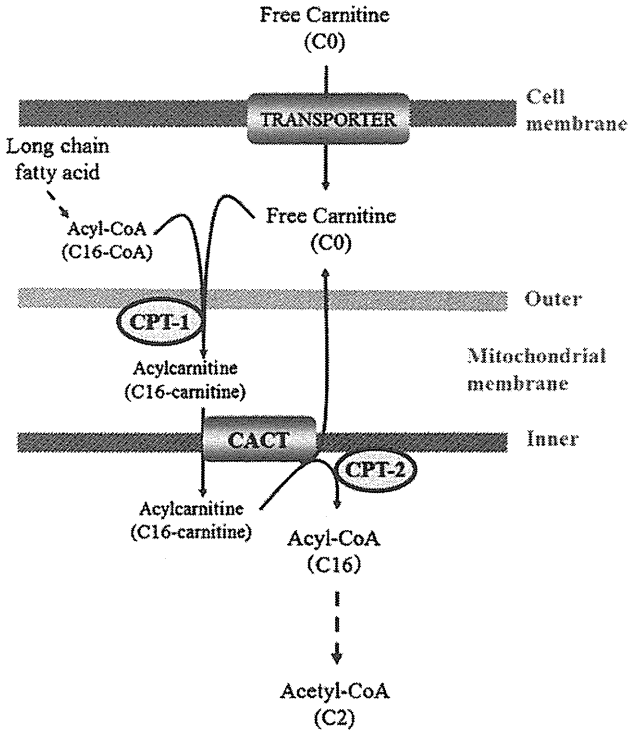

Fig. 1 Pathway for mitochondrial fatty acid beta-oxidation. Transporter: carnitine uptake transporter; *CPT-1*: carnitine palmitoyltransferase-1, *CACT*: carnitine acylcarnitine translocase, *CPT-2*: carnitine palmitoyltransferase-2. *Solid arrows* indicate single reactions; *dashed arrows* indicate multiple reactions or steps

encephalopathy, hepatomegaly, myopathy, hypoglycemia, and hyperammonemia, mainly result from low carnitine concentration in the tissues. On the other hand, secondary carnitine deficiency occurs in some conditions such as organic acidemias, renal dialysis, long-term medication (antiepileptic drugs or some antibiotics), and alimentary deficiency of L-carnitine [7–9].

It is necessary to make a differential diagnosis of PCD from the secondary carnitine deficiency or other false-positive cases, and diagnosis is confirmed by demonstrating reduced transport in skin fibroblasts from the patients. Until now, cluster-tray method using radioisotope-labeled substrate was used for the diagnosis of PCD [4, 10–12]. However, such a diagnostic method requires handling of radioactive substrates and focused only on diagnosis of PCD. Gene sequencing in SLC22A5 is one diagnostic method for PCD. However, it is molecularly heterogenous, and around 50 different mutations have been identified [6]. After acylcarnitine analysis using tandem MS analysis became available in the worldwide, blood acylcarnitine analysis was used as an initial method for diagnosis of FAO disorders and a detection of FAO disorders has been increased. However, it is necessary to confirm the diagnosis of the diseases with detailed analysis. The in vitro probe acylcarnitine (IVP) assay using cultured fibroblasts and tandem mass spectrometry (MS/MS) has been used to evaluate FAO capacity in the cultured cells and make a diagnosis of FAO disorders [13–15]. However, conventional IVP assay is not feasible to diagnose PCD or CPT1 deficiency, because excess amount of free carnitine is added to the experimental medium at the beginning. Estimation of free carnitine, which is the key marker for the above diseases, in experimental medium was nonsense for diagnosis of these disorders. We developed a novel functional assay for PCD and CPT1 deficiency using the IVP assay, with some modifications. This method uses different concentrations of exogenous free carnitine and measures intracellular as well as extracellular acylcarnitine (AC) levels, which overcomes the disadvantage of the conventional IVP assay in the diagnosis of carnitine cycle disorders.

Materials and methods

Materials

Hexanoylcarnitine (C6), octanoylcarnitine (C8), decanoylcarnitine (C10), and palmitoylcarnitine (C16) were purchased from Sigma–Aldrich (St Louis, MO, USA). Methanol, acetonitrile, and formic acid were purchased from Wako (Osaka, Japan). As an internal standard, a labeled carnitine standard kit (NSK-B), which contains $^{2}[H]_{9}$-carnitine, $^{2}[H]_{3}$-acetylcarnitine, $^{2}[H]_{3}$-propionylcarnitine, $^{2}[H]_{3}$-butyrylcarnitine, $^{2}[H]_{9}$-isovalerylcarnitine, $^{2}[H]_{3}$-octanoylcarnitine, $^{2}[H]_{9}$-myristoylcarnitine, and $^{2}[H]_{3}$-palmitoylcarnitine, was purchased from Cambridge Isotope Laboratories (Andover, MA, USA).

Preparation of standard solutions of ACs

Standard solutions containing 1, 10, 25, and 50 μmol/L each of C6, C8, C10, and C16 were used to validate the recovery and determine linear concentration range of ACs after extraction by the Folch method [16]. The ACs were dissolved in methanol (99.8 %), and the prepared standard solution was analyzed directly and after extraction by the Folch method.

Subjects

Human skin fibroblasts from six healthy controls (volunteers) and seven patients with various carnitine cycle disorders—three each with PCD and CPT2 deficiency and one with CPT1 deficiency—were analyzed. In all cases, diagnoses were confirmed by mass spectrometric analyses (gas chromatography-mass spectrometry and MS/MS), enzyme assay, and protein or mutational analyses. Informed consent was obtained from the patients or their families. This study was approved by the Ethical Committee of the Shimane University School of Medicine.

In vitro probe acylcarnitine (IVP) assay using MS/MS

An IVP assay was performed, as described, with some modifications [13, 15, 17], and principle of IVP assay was shown Fig. 2. Briefly, 3×10^6 cells were seeded in triplicate onto a six-well microplate (35 mm i.d.; Iwaki) and cultured until confluent. After washing twice with Dulbecco's phosphate buffered saline (DPBS; Invitrogen, Carlsbad, CA, USA), the cells were subsequently cultured for 96 h in 1 ml of a special experimental minimal essential medium (MEM) containing bovine serum albumin (0.4 % essential fatty acid-free BSA; Sigma), two different concentrations of C0 (Sigma)—10 μmol/L (reduced level, lower compared with physiological level) and 400 μmol/L (excess level)—and unlabelled palmitic acid (0.2 mmol/L; Nacalai Tesque). C0 and AC levels in the culture medium (extracellular fraction) and in the intracellular extract were analyzed after a 96-h incubation period using MS/MS (API 3000; Applied Biosystems, Foster City, CA, USA), as described [18].

Intracellular acylcarnitine extraction

Intracellular C0 and ACs were extracted using the Folch method, with some modification [16]. Briefly, harvested cells were washed twice with DPBS buffer. The cell pellet was resuspended in 100 μl volume of DPBS buffer and immediately frozen in liquid N_2. In order to separate phospholipids and cell debris, 250 μl of Folch reagent (chloroform/methanol, 2:1) was added to the resuspended cell pellet. After vigorous mixing using a vortex mixer, the solution was centrifuged for 10 min at 15,000 rpm at 4 °C. The debris layer around the interface between the aqueous and lipid phases was removed, and the extracted aqueous and lipid phases were mixed and thereafter dried under a nitrogen stream at 50 °C. ACs in culture medium supernatants and extracted intracellular ACs lysate were analyzed using MS/MS (API 3000; Applied Biosystems, Foster City, CA, USA). Briefly, methanol (200 μl) including an isotopically labeled internal standard (Cambridge Isotope Laboratories, Kit NSK-A/B, Cambridge, UK) was added to 10 μL of supernatant from culture medium and extracted intracellular ACs, for 30 min. Portions were centrifuged at 1,000×*g* for 10 min, and then 150 μL of supernatant was dried under a nitrogen stream and butylated with 50 μL of 3 N *n*-butanol-HCl at 65 °C for 15 min. The dried butylated sample was dissolved in 100 μL of 80 % acetonitrile/water (4:1 *v/v*), and then the ACs in 10 μL of the aliquots were determined using MS/MS [18] and quantified using Chemo-View™ software (Applied Biosystems/MDS SCIEX, Toronto, Canada).

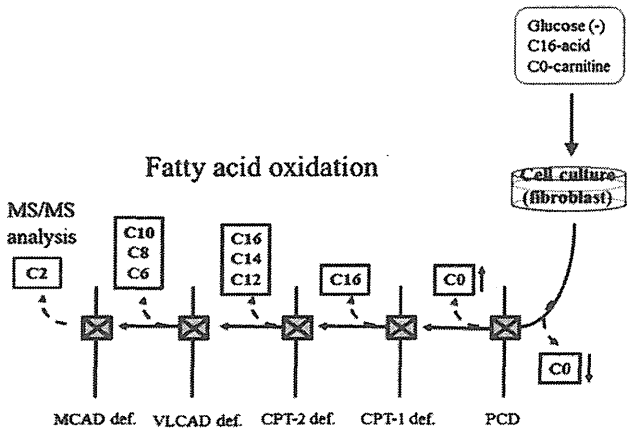

Fig. 2 Principle of in vitro probe acylcarnitine assay. *C2, C4, C6, C8, C10, C12, C14*, and *C16* represent acylcarnitines

Protein concentration and cell viability

Protein concentrations were measured by a modification of the Bradford method using the Bio-Rad protein assay (Bio-Rad, Hercules, CA, USA) [19]. The percentage of viable cells was determined at 24, 48, 72, and 96 h of incubation using the modified 3-(4,5-dimethyl-2-yl)-2, 5-diphenyl-2H-tetrazolium bromide (MTT) assay [20].

Data and statistical analysis

The results are expressed as mean±SD from at least three independent experiments for IVP assay in each cultured cell and three intra-assays and three inter-assays for recovery of standard AC solutions, and statistical significance was evaluated using Student's *t*test in Microsoft Excel. The AC concentrations were expressed as nanomoles per milligram protein.

Results

Recovery of ACs during Folch extraction

The AC standards in the aqueous or lipid fraction were analyzed separately using MS/MS, after extraction by the Folch procedure, and compared with direct analysis of the total mixed standard solutions using three inter-assays and three intra-assays of analysis of standard AC solution. As shown in Fig. 3, most of the C6 and C8-carnitines fractionated to the aqueous phase, while almost all C16-carnitine was exclusively retained in the lipid phase. The amount of C10-carnitine was comparable in both aqueous and lipid phases.

To determine the loss of C0 and ACs during Folch extraction, the standard AC solution was analyzed directly after routine sample preparation for MS/MS and compared with that after Folch extraction. The recovery of ACs in the

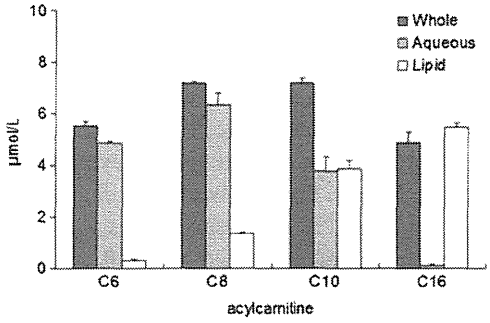

Fig. 3 Recovery of ACs during extraction using the Folch method. Standard solutions of 10 μmol/L each of C6-, C8-, C10-, and C16-carnitine were used to determine the recovery of ACs in the aqueous and lipid fractions during extraction using the Folch method. *Grey column*: ACs in the whole extract after Folch method; *striped column*: ACs in the aqueous fraction of Folch extraction; *open column*: ACs in lipid fraction of Folch extraction. Data are expressed as mean±SD (micromoles per liter) from three intra-assays and three inter-assays, and statistical significance was evaluated using Student's *t*test in Microsoft Excel

standard solutions after direct analysis and Folch extraction procedure was analyzed three times by inter-assay. The inter-assay CV of acylcarnitines ranged from 3.21 to 8.33 %. No statistical difference was seen between direct analysis and after Folch extraction.

Acylcarnitine profile in extracellular medium of cultured fibroblasts with excess and reduced concentrations of free carnitine

Using fibroblasts from various carnitine cycle disorders, AC profiles were determined in the extracellular medium with reduced or excess concentration of C0. Reported conventional IVP assay used excess levels of C0 (400 μmol/L) [14, 15, 17, 21]. With excess amount of C0 (Table 1, "Medium (C0-excess, 400 μM)"), a selective increase in C16 and a decrease in acetylcarnitine (C2) was observed in cases of CPT2-deficient fibroblasts. AC profiles in media from PCD- and CPT1-deficient fibroblasts were similar to that of healthy controls. In PCD fibroblasts, C2 was 53.1 % of the normal control while C2 in CPT1-deficient fibroblasts was 140 % of the normal control. No statistical difference in C0 level was observed among CPT2-, PCD-, and CPT1-deficient fibroblasts and a healthy control.

In the extracellular medium containing reduced C0, C16 remains higher in cells with CPT2 deficiency, while AC profiles were similar to those observed in C0-excess for PCD- and CPT1-deficient cells and the healthy controls (Table 1, "Medium (C0-reduced, 10 μM)").

Acylcarnitine profile in intracellular lysate with various concentrations of free carnitine

The intracellular C0 and ACs were measured after AC extraction using the Folch method. C16 in the intracellular lysate from CPT2-deficient fibroblasts was significantly elevated in both reduced and excess C0 conditions similar to those in extracellular medium, and diagnostic significant was kept. In the excess C0 condition, CPT1- and PCD-deficient fibroblasts could not be distinguished clearly; based on the C0 levels, even C16 level was relatively low (Fig. 4a). On the other hand, the intracellular C0 under conditions with reduced C0 was 41.78±1.47 and 6.31± 2.88 nmol/mg protein/96 h in the normal controls (n=6) and patients with PCD (n=3), respectively, and the C0 levels of PCD cells were significantly lower (p<0.001) as shown in Fig. 4b. This indicated that the C0 uptake was significantly decreased in PCD compared with control in

Table 1 Acylcarnitine profiles of in vitro probe acylcarnitine assay

	Acylcarnitines, nmol/mg protein/96 h						
	C0	C2	C6	C8	C12	C14	C16
Medium (C0 excess, 400 μM)							
Control (n=6)	411.74±23.08	11.80±1.54	2.60±0.09	1.70±0.47	0.79±0.22	0.34±0.19	2.06±0.77
PCD (n=3)	432.18±18.76	6.25±0.96	2.09±0.40	0.94±0.54	0.41±0.33	0.20±0.10	1.72±0.57
CPT-1 (n=1)	357.69±34.16	16.52±5.60	1.73±0.87	0.54±0.94	0.18±0.14	0.17±0.16	1.36±0.98
CPT-2 (n=3)	376.56±42.71	6.88±0.72	0.94±0.65	0.41±0.22	1.70±0.35	0.80±0.05	18.73±1.07
Medium (C0 reduced, 10 μM)							
Control (n=6)	9.85±0.30	1.70±0.74	0.78±0.30	0.18±0.09	0.10±0.08	0.03±0.01	0.51±0.11
PCD (n=3)	10.03±0.71	0.74 ±0.33	0.75±0.31	0.06±0.04	0.03±0.01	0.01±0.01	0.20±0.08
CPT-1 (n=1)	11.06±0.75	7.56±3.10	0.98±0.30	0.55±0.62	0.09±0.09	0.08 ±0.07	0.01 ±0.02
CPT-2 (n=3)	9.73±1.94	0.64±0.23	0.54±0.20	0.11±0.03	0.22±0.06	0.04±0.01	2.79±0.38

The results are expressed as mean±SD from three independent experiments with triplication in each cell line. The AC concentration was expressed as nanomoles per milligram protein. *C0* free carnitine, *C2* acetylcarnitine, *C6* hexanoylcarnitine, *C8* octanoylcarnitine, *C12* dodecanoylcarnitine, *C14* myristoylcarnitine, *C16* palmitoylcarnitine

C0-reduced condition. Concentration of C16 was also significantly low in PCD in C0-reduced condition. Under the C0-reduced condition, intracellular C0 was much higher, but C16 was much lower in CPT1-deficient fibroblasts, compared with the levels in controls (Fig. 4b).

The ratio of intracellular C0 to extracellular C0 in PCD was significantly lower than that of the controls ($p<0.001$) in the C0-reduced condition, while that in C0-excessive condition was not significantly different (Fig. 5). Cell viability was measured using the MTT assay under reduced or excess concentrations of C0. The percentage of viable cells cultured in C0-reduced medium was equivalent to that in C0-excess media (data not shown).

Discussion

The present study developed a novel IVP assay for the accurate diagnosis of PCD and CPT1 deficiency. Although previous studies reported that IVP assay was a powerful method for the diagnosis of most FAO disorders [13, 14, 21], this assay turned out to be unable to identify PCD and CPT1 deficiencies. At first, we used a C0-excess experimental medium, which contained 400 μmol/L of C0, according to previous reports [13, 14, 21]. Extracellular

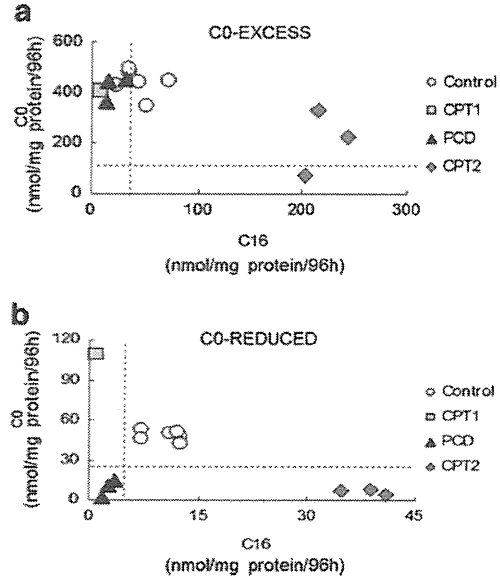

Fig. 4 Intracellular C0 and C16 correlation in patients with carnitine cycle disorders. **a** C0-excessive condition (−*E*); **b** C0-reduced condition (−*R*). *open circle*: healthy control ($n=6$); *closed triangle*: PCD ($n=3$); *closed square*: CPT1 deficiency ($n=1$); *closed diamond*: CPT2 deficiency ($n=3$). Cells were incubated in experimental medium with 400 or 10 μmol/L of free carnitine and 200 μmol/L of palmitic acid. After 96-h incubation, cells were harvested, and intracellular free carnitine (C0) and palmitoylcarnitine (C16) were extracted using Folch method and measured using MS/MS. Data of mean values of triplicates are presented (nanomoles per milligram protein per 96 h)

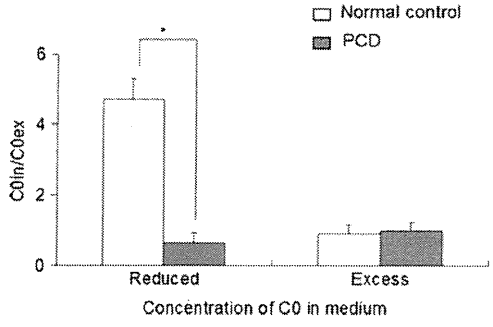

Fig. 5 Ratio of intracellular C0 to extracellular C0. *Open square*: normal control ($n=6$); *closed square*: PCD ($n=3$). Extra- and intracellular C0 of cells with normal control and PCD were measured in C0-reduced (10 μmol/L) and C0-excess (400 μmol/L) conditions using MS/MS. Data are expressed as mean±SD of six normal controls and three patients with PCD. Experiment in each cell line was repeated twice with triplications. Significant differences between normal control and PCD are shown as $*p<0.001$

AC profiles of patients with PCD and CPT1 deficiency showed a pattern similar to that of normal controls by the conventional assay that contains excessive C0 (400 μmol/L) in the culture medium, since C0 moves across the cell membrane down its concentration gradient by passive diffusion. Long-chain fatty acids are transferred across the inner mitochondrial membrane with the assistance of carnitine and carnitine cycle enzymes. The subsequent FAO functions normally even in PCD, and AC profile in PCD is similar to that in normal FAO. Next, we used 50 μmol/L of C0 because the normal range of free carnitine in human plasma was approximately 25 to 50 μmol/L [6]. However, there was no diagnostic difference compare with C0-excess condition, and data are not shown. We analyzed IVP assay in C0-deficient condition (10 μmol/L of C0).

It is known that fibroblasts and muscle and cardiac cells have a high-affinity, low-capacity transporter system [22], and carnitine concentrations in the tissues are much higher than those in serum [23]. Analysis of intracellular C0 and ACs is more relevant for the diagnosis of PCD and CPT1 deficiency because it was shown that C0 was decreased in PCD and increased in CPT1 deficiency in those tissues. When we analyzed cell lysates with MS/MS after direct sonication, artificial peaks of ACs were detected, and the background peaks of mass spectrum were high and hampered the subsequent analyses (data not shown). Hence, we extracted intracellular ACs using a modified Folch method and analyzed both the intracellular lysate and the extracellular medium. This allowed visualization of clear peaks of C0 and ACs in the intracellular lysate, validating that the Folch extraction can be used for simultaneous quantitation of intracellular C0 and a wide range of ACs (short- to long-chain AC).

Uptake of C0 and abnormalities in ACs were associated with the concentration of C0 in culture medium. In the C0-excess condition, it was hard to differentiate PCD from control

cells. Levels of C0 and C16 were overlapped with those of normal control. On the other hand, in the C0-reduced condition, intracellular C0 was significantly decreased in PCD while being increased in CPT1 deficiency, compared with that in normal control. C0-reduced medium was changed after fibroblasts equilibrated in MEM, and normal control could force to uptake free carnitine in C0-deficient condition while cells with PCD could not uptake sufficiently in that condition. Furthermore, the following fatty acid oxidation cycle interrupted, and C16 also decreased in PCD. This correlation of C0 and C16 in the C0-reduced condition is more informative for the diagnosis of carnitine cycle disorders (Fig. 4b). Since cells with PCD cannot uptake C0 via the cell membrane, the finding of reduction of both C0 and C16 is specific for PCD. In case of CPT1 deficiency, C0 uptake is normal, but it cannot bind acyl-CoA ester, resulting in reduced long-chain acylcarnitine production, and FAO is disturbed. Therefore, the stored intracellular ACs were consumed by FAO, and intracellular C16 as well as total ACs were decreased, and C0 was accumulated in intracellular lysate. In contrast, the AC profile of low level of C0 and high level of C16 is diagnostic for CPT2 deficiency. In this disease, normally transferred long-chain AC cannot be converted back from ACs to acyl-CoA esters and C0, the substrate for FAO. Additionally, the ratio of intracellular and extracellular C0s can sensitively distinguish PCD from control in the C0-reduced medium because carnitine transporter of normal cells was forced to uptake C0 up to physiological level in C0-reduced condition while cells with PCD failed for it. In excessive C0 condition, ratio of intracellular and extracellular C0 was similar to that in normal control and PCD since C0 transfer by passive diffusion across the cell membrane.

In conclusion, the simultaneous analysis of intracellular and extracellular C0 and ACs under the various concentrations of free carnitine in the culture medium is useful for diagnosis of FAO, especially carnitine cycle disorders. This study confirms that the newly modified IVP assay is an easy and safe method to diagnose PCD and CPT1 deficiency.

Acknowledgments We thank all the attending physicians for providing clinical information regarding each patient. We are also grateful to Y. Ito, M. Furui, T. Esumi, and N. Tomita for their technical assistance. This work was supported by a Grant-in-Aid for scientific research from the Japan Society for the Promotion of Science (J.P., and S.Y.) and a Grant from the Ministry of Education, Science, Technology, Sports and Culture of Japan and the Ministry of Health, Labour and Welfare of Japan (S.Y).

References

1. McGarry JD, Brown NF (1997) The mitochondrial carnitine palmitoyltransferase system. From concept to molecular analysis. Eur J Biochem 244:1–14
2. Sim KG, Hammond J, Wilcken B (2002) Strategies for the diagnosis of mitochondrial fatty acid beta-oxidation disorders. Clin Chim Acta 323:37–58
3. Tamai I, Ohashi R, Nezu J, Yabuuchi H, Oku A et al (1998) Molecular and functional identification of sodium ion-dependent, high affinity human carnitine transporter OCTN2. J Biol Chem 273:20378–20382
4. Treem WR, Stanley CA, Finegold DN, Hale DE, Coates PM (1988) Primary carnitine deficiency due to a failure of carnitine transport in kidney, muscle, and fibroblasts. N Engl J Med 319:1331–1336
5. Eriksson BO, Gustafson B, Lindstedt S, Nordin I (1989) Transport of carnitine into cells in hereditary carnitine deficiency. J Inherit Metab Dis 12:108–111
6. Longo N, di San A, Filippo C, Pasquali M (2006) Disorders of carnitine transport and the carnitine cycle. Am J Med Genet C Semin Med Genet 142C:77–85
7. Nakajima Y, Ito T, Maeda Y, Ichiki S, Sugiyama N et al (2010) Detection of pivaloylcarnitine in pediatric patients with hypocarnitinemia after long-term administration of pivalate-containing antibiotics. Tohoku J Exp Med 221:309–313
8. Hori T, Fukao T, Kobayashi H, Teramoto T, Takayanagi M et al (2010) Carnitine palmitoyltransferase 2 deficiency: the time-course of blood and urinary acylcarnitine levels during initial L-carnitine supplementation. Tohoku J Exp Med 221:191–195
9. Tein I, DiMauro S, Xie ZW, De Vivo DC (1993) Valproic acid impairs carnitine uptake in cultured human skin fibroblasts. An in vitro model for the pathogenesis of valproic acid-associated carnitine deficiency. Pediatr Res 34:281–287
10. Pons R, Carrozzo R, Tein I, Walker WF, Addonizio LJ et al (1997) Deficient muscle carnitine transport in primary carnitine deficiency. Pediatr Res 42:583–587
11. Scaglia F, Wang Y, Longo N (1999) Functional characterization of the carnitine transporter defective in primary carnitine deficiency. Arch Biochem Biophys 364:99–106
12. Wang Y, Ye J, Ganapathy V, Longo N (1999) Mutations in the organic cation/carnitine transporter OCTN2 in primary carnitine deficiency. Proc Natl Acad Sci U S A 96:2356–2360
13. Endo M, Hasegawa Y, Fukuda S, Kobayashi H, Yotsumoto Y et al (2010) In vitro probe acylcarnitine profiling assay using cultured fibroblasts and electrospray ionization tandem mass spectrometry predicts severity of patients with glutaric aciduria type 2. J Chromatogr B Analyt Technol Biomed Life Sci 878:1673–1676
14. Law LK, Tang NL, Hui J, Ho CS, Ruiter J et al (2007) A novel functional assay for simultaneous determination of total fatty acid beta-oxidation flux and acylcarnitine profiling in human skin fibroblasts using (2)H(31)-palmitate by isotope ratio mass spectrometry and electrospray tandem mass spectrometry. Clin Chim Acta 382:25–30
15. Okun JG, Kolker S, Schulze A, Kohlmuller D, Olgemoller K et al (2002) A method for quantitative acylcarnitine profiling in human skin fibroblasts using unlabelled palmitic acid: diagnosis of fatty acid oxidation disorders and differentiation between biochemical phenotypes of MCAD deficiency. Biochim Biophys Acta 1584:91–98
16. Jauregui O, Sierra AY, Carrasco P, Gratacos E, Hegardt FG et al (2007) A new LC-ESI-MS/MS method to measure long-chain acylcarnitine levels in cultured cells. Anal Chim Acta 599:1–6
17. Ventura FV, Costa CG, Struys EA, Ruiter J, Allers P et al (1999) Quantitative acylcarnitine profiling in fibroblasts using [U-13C] palmitic acid: an improved tool for the diagnosis of fatty acid oxidation defects. Clin Chim Acta 281:1–17
18. Li H, Fukuda S, Hasegawa Y, Kobayashi H, Purevsuren J et al (2010) Effect of heat stress and bezafibrate on mitochondrial beta-oxidation: comparison between cultured cells from normal and mitochondrial fatty acid oxidation disorder children using in vitro probe acylcarnitine profiling assay. Brain Dev 32:362–370

19. Bradford MM (1976) A rapid and sensitive method for the quantitation of microgram quantities of protein utilizing the principle of protein-dye binding. Anal Biochem 72:248–254
20. Honma Y, Ishii Y, Yamamoto-Yamaguchi Y, Sassa T, Asahi K (2003) Cotylenin A, a differentiation-inducing agent, and IFN-alpha cooperatively induce apoptosis and have an antitumor effect on human non-small cell lung carcinoma cells in nude mice. Cancer Res 63:3659–3666
21. Schulze-Bergkamen A, Okun JG, Spiekerkotter U, Lindner M, Haas D et al (2005) Quantitative acylcarnitine profiling in peripheral blood mononuclear cells using in vitro loading with palmitic and 2-oxoadipic acids: biochemical confirmation of fatty acid oxidation and organic acid disorders. Pediatr Res 58:873–880
22. Tein I, De Vivo DC, Bierman F, Pulver P, De Meirleir LJ et al (1990) Impaired skin fibroblast carnitine uptake in primary systemic carnitine deficiency manifested by childhood carnitine-responsive cardiomyopathy. Pediatr Res 28:247–255
23. Stanley CA (1987) New genetic defects in mitochondrial fatty acid oxidation and carnitine deficiency. Adv Pediatr Infect Dis 34:59–88

Molecular Genetics and Metabolism 110 (2013) 42–53

Contents lists available at ScienceDirect

Molecular Genetics and Metabolism

journal homepage: www.elsevier.com/locate/ymgme

Minireview

Newborn screening and diagnosis of mucopolysaccharidoses

Shunji Tomatsu [a,*], Tadashi Fujii [b], Masaru Fukushi [b], Toshihiro Oguma [c], Tsutomu Shimada [a], Miho Maeda [a], Kazuhiro Kida [d], Yuniko Shibata [e], Hideyuki Futatsumori [e], Adriana M. Montaño [f], Robert W. Mason [a], Seiji Yamaguchi [g], Yasuyuki Suzuki [h], Tadao Orii [i]

[a] Nemours/Alfred I. duPont Hospital for Children, Wilmington, DE, USA
[b] Sapporo IDL, Sapporo, Japan
[c] Translational Medicine & Clinical Pharmacology Department, Daiichi Sankyo Co., Tokyo, Japan
[d] Clinical Laboratory Medicine, National Center for Child Health and Development, Tokyo, Japan
[e] Central Research Lab., R&D Div. Seikagaku Co., Tokyo, Japan
[f] Department of Pediatrics, Saint Louis University, St. Louis, MO, USA
[g] Department of Pediatrics, Shimane University, Izumo, Japan
[h] Medical Education Development Center, Gifu University, Japan
[i] Department of Pediatrics, Gifu University, Gifu, Japan

ARTICLE INFO

Article history:
Received 4 May 2013
Received in revised form 5 June 2013
Accepted 6 June 2013
Available online 21 June 2013

Keywords:
Mucopolysaccharidoses
Tandem mass spectrometry
Newborn screening
Glycosaminoglycans
Monitoring

ABSTRACT

Mucopolysaccharidoses (MPS) are caused by deficiency of lysosomal enzyme activities needed to degrade glycosaminoglycans (GAGs), which are long unbranched polysaccharides consisting of repeating disaccharides. GAGs include: chondroitin sulfate (CS), dermatan sulfate (DS), heparan sulfate (HS), keratan sulfate (KS), and hyaluronan. Their catabolism may be blocked singly or in combination depending on the specific enzyme deficiency. There are 11 known enzyme deficiencies, resulting in seven distinct forms of MPS with a collective incidence of higher than 1 in 25,000 live births. Accumulation of undegraded metabolites in lysosomes gives rise to distinct clinical syndromes. Generally, the clinical conditions progress if untreated, leading to developmental delay, systemic skeletal deformities, and early death. MPS disorders are potentially treatable with enzyme replacement therapy or hematopoietic stem cell transplantation. For maximum benefit of available therapies, early detection and intervention are critical. We recently developed a novel high-throughput multiplex method to assay DS, HS, and KS simultaneously in blood samples by using high performance liquid chromatography/tandem mass spectrometry for MPS. The overall performance metrics of HS and DS values on MPS I, II, and VII patients vs. healthy controls at newborns were as follows using a given set of cut-off values: sensitivity, 100%; specificity, 98.5–99.4%; positive predictive value, 54.5–75%; false positive rate, 0.62–1.54%; and false negative rate, 0%. These findings show that the combined measurements of these three GAGs are sensitive and specific for detecting all types of MPS with acceptable false negative/positive rates. In addition, this method will also be used for monitoring therapeutic efficacy. We review the history of GAG assay and application to diagnosis for MPS.

Contents

Abbreviations: CS, chondroitin sulfate; CF, cystic fibrosis; CNS, central nervous system; CPC, cetylpyridinium chloride; DBS, dried blood spot; DMB, dimethylmethylene blue; DS, dermatan sulfate; ERT, enzyme replacement therapy; ESI-MS/MS, electrospray ionization tandem mass spectrometry; GAG, glycosaminoglycans; GALNS, N-acetylgalactosamine-6-sulfate sulfatase; GUS, β-glucuronidase; HPLC, high performance liquid chromatography; HS, heparan sulfate; HSCT, hematopoietic stem cell transplantation; KS, keratan sulfate; LC–MS/MS, high performance liquid chromatography tandem mass spectrometry; MPS, mucopolysaccharidoses; NBS, newborn screening; SRT, substrate reduction therapy.

* Corresponding author at: Skeletal Dysplasia Center, Nemours Biomedical Research, Nemours/Alfred I. duPont Hospital for Children, 1600 Rockland Rd., Wilmington, DE 19899-0269, USA. Fax: +1 302 651 6888.
E-mail address: stomatsu@nemours.org (S. Tomatsu).

1096-7192/$ – see front matter © 2013 Elsevier Inc. All rights reserved.
http://dx.doi.org/10.1016/j.ymgme.2013.06.007

1. Introduction

Mucopolysaccharidoses (MPS) are caused by deficiency of lysosomal enzyme activities needed to degrade glycosaminoglycans (GAGs), which are long unbranched polysaccharides consisting of repeating disaccharides [1]. GAGs include: chondroitin sulfate (CS), dermatan sulfate (DS), heparan sulfate (HS), keratan sulfate (KS), and hyaluronan. Their catabolism is inhibited singly or in combination depending on the specific enzyme deficiency. Lysosomal accumulation of GAG molecules results in cell, tissue, and organ dysfunction. In MPS, the undegraded or partially degraded GAGs are stored in lysosomes and/or secreted into the blood stream and subsequently excreted in urine. There are 11 known enzyme deficiencies that give rise to seven distinct MPS.

The MPS share many clinical features, although to variable degrees. Most MPS patients are asymptomatic at birth, with subsequent onset of clinical signs and symptoms. These clinical features include a chronic and progressive disease course, multiple organ system involvement, organomegaly, dysostosis multiplex, and abnormal facies. Hearing, vision, and cardiopulmonary functions are affected. Profound neurological impairment is characteristic of MPS I (Hurler syndrome), the severe form of MPS II (Hunter syndrome), and all subtypes of MPS III (Sanfilippo syndrome). MPS IV (Morquio syndrome) and MPS VI (Maroteaux–Lamy syndrome) have characteristic bone lesions without central nervous system (CNS) involvement. There is clinical similarity between different enzyme deficiencies and, conversely, a wide spectrum of clinical severity within any one enzyme deficiency [1]. In all cases, except for a few mild cases, the disease is ultimately fatal with an average life expectancy of one to two decades if untreated. MPS can be found worldwide. Although the overall incidence of MPS is estimated as higher than 1:25,000 live births, the incidence of a particular type of MPS varies (Table 1) [2–8]. Scott et al. (2013) showed that in a pilot study of 110,000 dried blood spot (DBS), the incidence of MPS I is 1 in 35,700 [9].

We estimate that approximately 200 newborns affected with MPS are born annually in the United States.

The stepwise degradation of GAGs requires four exoglycosidases, five sulfatases, and one nonhydrolytic transferase. One endoglycosidase also participates in the degradation [10]. Understanding the degradation of GAGs is relevant to establishing new screening methods and monitoring therapies. The backbone of the CS chain consists of repetitive disaccharide units containing D-glucuronic acid (GlcA) and N-acetylgalactosamine (GalNAc) residues, whereas DS is a stereoisomeric variant of CS with varying proportions of L-iduronic acid (IdoA) in place of GlcA. CS and DS are involved in cell adhesion and neuritogenesis [11]. The HS-GAG chains are linear polysaccharides composed of alternating *N*-acetylated or *N*-sulfated glucosamine units (N-acetylglucosamine, GlcNAc, or *N*-sulfoglucosamine, GlcNS) and uronic acids (GlcA or IdoA). HS is involved in diverse biologic functions including activation of growth factors [11]. The backbone of the KS chain consists of repetitive disaccharide units containing lactosamine, which is composed of galactose (Gal) and GlcNAc residues. KS is involved in cell motility, embryo implantation, wound healing, corneal transparency, extracellular matrix of cartilage, and neuronal regeneration [12].

Therapies for MPS have been developed experimentally and clinically. These include hematopoietic stem cell transplantation (HSCT), enzyme replacement therapy (ERT), gene therapy, and substrate reduction therapy (SRT), all of which lead to the partial restoration of the enzyme activity or inhibition of GAG synthesis. HSCT is not entirely effective and has a relatively high mortality rate, primarily from graft versus host disease [13,14]. Treating MPS with ERT relies on the cellular uptake of the enzyme by receptor-mediated endocytosis. ERT has been quite successful in animal models, leading to application in human patients [15–19]. ERT is FDA approved for use in patients with MPS I [20], MPS II [21,22], and MPS VI [23–26]. Patients treated with ERT demonstrate clinical improvement of somatic manifestations and quality of life. Trials for MPS IVA and other types of MPS are under way. While ERT holds much promise for the treatment of MPS, current experience with MPS animal models indicates that it is unlikely that therapeutic amounts of enzyme: 1) cross the blood brain barrier to correct the CNS pathology and 2) reach the bone cells to correct the skeletal pathology. Experimental gene therapies and SRT are under way in vivo [27–29].

Table 1
Mucopolysaccharidoses and GAG storage [1–9].

Disorder	Deficient	Incidence	Primary storage material
MPS I	α-L-Iduronidase	1/35,700	DS, HS
MPS II	Iduronate-2-sulfatase	1/93,000–200,000	DS, HS
MPS IIIA	Heparan-N-sulfatase	1/5,3000–370,000	HS
MPS IIIB	α-N-acetylglucosaminidase		HS
MPS IIIC	Acetyl-CoA:α-glucosaminide acetyltransferase		HS
MPS IIID	N-acetylglucosamine 6-sulfatase		HS
MPS IVA	N-acetylgalactosamine-6-sulfate sufatase	1/7,6000–1,428,000	C6S. KS
MPS IVB	β-Galactosidase		KS
MPS VI	N-acetylgalactosamine-4-sulfatase	1/207,000–2,000,000	C4S, DS
MPS VII	β-D-Glucuronidase	1/345,000–2,100,000	C4, 6S, DS, HS,

The most commonly used methods for diagnosis of MPS are dye-spectrometric methods such as dimethylmethylene blue (DMB) [30–32] and alcian blue [33–35] on urine samples. The direct DMB method was automated for detection of MPS diseases [32]. However, these methods cannot be applied to blood specimens without prior protease, nuclease, or hyaluronidase digestion and are impractical for screening newborn urine since collection is difficult and storage of large volumes of urine samples is costly. These spectrometric assays are also not adequate for screening: 1) proteins in the blood specimen block binding of the dyes to GAG, 2) the staining dyes are prone to decomposition leading to a low signal to noise ratio, and 3) the dye methods cannot predict MPS subtypes. HPLC is a sensitive and specific method but not appropriate for mass screening since it is time-consuming and expensive [36–40]. Although sandwich ELISA methods to measure specific GAGs such as HS and KS have been developed to detect MPS [41–43], a method to detect DS is not available.

A suitable method for newborn screening (NBS) must be inexpensive and should be performed on DBS from a Guthrie card. Two other potential methods have been proposed [44]. One is an immune-capture method for detecting each deficient lysosomal protein from patients with MPS I, MPS II, MPS IIIA, and MPS VI [45,46], and the other one is a direct method, assaying individual enzyme activities for MPS I, MPS II, MPS IIIB, MPS IVA, MPS VI, and MPS VII patients [47–55]. These approaches, which rely on individual antibodies or enzyme activities for first-tier screening, are still being developed to detect all types of MPS. We have developed multiplex assays for three MPS-associated metabolites that make NBS possible. Since cost-performance is an important key to applicability, highly efficient and inexpensive screening methodologies must be formulated and developed. Otherwise, the cost of screening for each type of MPS would be unacceptable, as the incidence ranges from approximately 1:100,000 births to 1:2,000,000 births. However, screening for MPS as a group with a combined incidence of higher than 1:25,000 births would be comparable with other existing screening programs for genetic disorders such as phenylketonuria (1:14,000) and galactosemia (1:50,000). Therefore, strategies that enable the simultaneous detection of a group of MPS by LC–MS/MS method are feasible for NBS []. Most NBS methods measure elevated substrates in organic acidemias, urea cycle disorders, and cystic fibrosis (CF). A two-tier strategy is universally used for CF [59–62].

The method described here for MPS has another advantage in that it can be used to monitor therapeutic effect [63,64] and to predict clinical severity.

The goal of this review is to describe the potential of tandem mass spectrometry assay of GAGs for NBS and diagnosis of MPS.

2. Historical review for GAG assay

2.1. Total urine GAG assay

The measurement of total GAG excretion in urine is widely used as a biomarker for MPS [65–67]. Urine GAG analysis is a useful initial screening test for MPS and may be also helpful for monitoring treatment efficacy. Measurement of total urine GAGs can be performed quantitatively and qualitatively. Both are recommended as part of the evaluation of patients for MPS.

In 1971, Berman et al. proposed a spot test for MPS (termed the Ames MPS paper spot) based on Azure A dye staining of GAGs in urine spotted on paper [68]. In 1985, Huang et al. measured the uronic acid content of the precipitated GAGs from MPS patients and age-matched normal controls by using spectrophotometric analysis of samples treated with cetylpyridinium chloride (CPC) [69]. In healthy individuals, uronic acid/creatinine ratios decreased until age 20 years old and then remained low. Most patients with MPS IV had higher uronic acid/creatinine ratios than age-matched controls. This same group also suggested that the Ames MPS paper spot test was a potential approach to screen MPS patients from a high risk group with suspected clinical features [70].

At the same timing, 1,9-dimethylmethylene blue (DMB) has been used to quantitatively detect GAGs in urine from older children [71,72]. The DMB method also measures the total amount of GAG in urine. In 1989, Whitley et al. showed that this testing could be used as a potential screen for any MPS disorder [73–75] as the test measures levels of all GAG species on the urine spot. In 1991, JG de Jong et al. proposed that the DMB method is more reliable than the Ames MPS paper spot [76].

In 2000, Orii's group reported that two MPS II patients were diagnosed by screening urine spot samples from approximately 130,000 six-month-old infants in a Japanese population using the DMB method [77, personal communication from T. Orii]. This was the first practical demonstration that GAG measurements can be used to screen for MPS. The limitations of the method are 1) some substances that respond to DMB are found in a diaper, leading to around 3% of a false positive result and GAG/creatinine ratio is not stable until 4 days old, suggesting that we can apply this method to the urine samples from the 5th day newborns [77,78].

Other dye-based procedures such as the toluidine blue spot test [79] and the alcian blue spot test [80] have been evaluated for qualitative screening. Overall, spot tests suffer from a high incidence of false negative results [80] and cannot be applied to blood spot.

Elevated urinary GAG is normally specific for an MPS disorder; however, many patients have borderline or only slightly elevated urinary GAGs, especially those with MPS IV, resulting in false negatives in a screen [41,42,73,75,81,82]. Total urine GAG levels are also unlikely to reflect the clinical severity or predict the specific clinical signs and symptoms that might arise.

Thus, a traditional method for urine GAG is still used for a screening, when the subject is suspected as a clinically high risk group; however, it is not suitable for a general mass screening of newborns. The lack of adequate sensitivity, specificity, and reliability of these screening tests underscores the need for improved methods of GAG detection for MPS.

2.2. Assay for specific GAGs

Several methods have been described for detecting and monitoring specific GAGs in MPS.

2.2.1. Chromatography

In 1968, Orii described the measurement of urine GAG in normal male children by using CPC fractionation and column chromatography on Dowex 1X2, showing the compositions of each specific GAG in urine [83].

In 1980, Kimura et al. described the chemical structure of DS in the urine of a patient with MPS II through the analysis of disaccharide units. Urine was digested by chondroitinase ABC and the resultant disaccharides were separated on a Dowex 1 column [84]. In 1984, the same group fractionated urinary heparan sulfates ("HS") from two siblings with MPS IIIB by chromatography on Dowex 1 and Sephadex G-50 columns [85].

In 1985, Hopwood and Elliott used Dowex 1 column separation to show that urine from MPS IIID, IVA, and VI patients contained elevated levels of sulphated *N*-acetylhexosamines compared with urine from normal individuals [86]. In 1995, K Murata et al. digested heterogeneous sulfated HS isomers with specific HS-lyases, heparitinase I, and heparinase, and separated the resultant unsaturated disaccharides (ΔDi-SHS) by HPLC. The pattern of ΔDi-SHS obtained from that urine of a patient with MPS I indicated accumulation of unique urinary HS isomers in this MPS [87].

Enzymatic and chemical analyses of the structures of HS in the urine by patients with MPS III and II revealed that their non-reducing ends differ from each other and reflect the enzyme deficiency of the syndromes [88]. In addition to providing a new tool for the differential diagnosis of the MPS, these results bring new insights into the specificity of the heparitinases from *Flavobacterium heparinum*.

In 1998, Byers et al. used a combination of anion-exchange chromatography and 30–40% gradient polyacrylamide gel electrophoresis (gradient-PAGE) to purify and characterize urinary GAG from various MPS [65]. The urinary GAG from the different MPS displayed distinct patterns on gradient-PAGE, and further confirmation of MPS types and subtypes was demonstrated by an electrophoretic shift in the banding pattern after digestion with the appropriate MPS enzyme. They reported that each MPS disorder accumulates a unique spectrum of GAGs, with a non-reducing terminus that is specific for the deficient enzyme that causes each particular MPS disorder. The absolute correlation of the non-reducing terminal structure with a particular MPS and the availability of recombinant lysosomal enzymes provide the means for a rapid and accurate diagnosis of individual MPS.

Thus, qualitative urine-based testing methods can separate the various GAG species and thereby provide a starting path for differential diagnosis. GAGs are first isolated from the urine and then separated by thin layer chromatography or electrophoresis [69,70,89–92]. A GAG specific stain is used to visualize the GAGs and the relative position on the gel or plate is used to identify GAG types [93]. KS, the specific diagnostic GAG in patients with MPS IVA, can be difficult to separate and visualize by these methods and result in false negatives. Numerous methods, including electrophoresis and spectrophotometry, have been evaluated for the quantitative and/or qualitative analysis of urinary GAGs. However, all these methodologies are laborious, time-intensive, and non-specific [80].

2.2.2. ELISA

In 1988, the measurements of blood KS were accomplished using an inhibition ELISA by Thonar et al. [94]. His group measured blood KS level in healthy controls, suggesting that blood KS is age-dependent. In 2004, Tomatsu et al. developed a sandwich ELISA method for KS measurements, showing that KS levels in blood and urine of MPS IVA patients are markedly elevated and that clinical severity correlates with the levels of blood and urine KS [41,42]. In 2005, Tomatsu et al. demonstrated that blood KS is elevated in other types of MPS, suggesting the potential of use of blood KS for screening and monitoring other types of MPS patients in addition to MPS IV. In the same year, Tomatsu et al. developed a sandwich ELISA method for HS measurement and showed that blood and urine HS levels are elevated in MPS I, II, III, VI, and VII patients and correlate with clinical severity [43]. The results of these studies indicate that blood and urine KS and HS measurements could be used as a biomarker for assessing clinical severity at an early stage, and to monitor therapeutic effects [95]. ELISAs to measure KS, HS, or DS are not available commercially.

2.2.3. Tandem mass spectrometry (MS/MS)

In 2003, Ramsay et al. developed a method for the derivatization and quantification of sulfated *N*-acetylhexosamine-containing mono- and disaccharides from patient samples by electrospray ionization tandem mass spectrometry (ESI-MS/MS) [96]. Urine from most MPS types had significant increases in mono- and di-sulfated *N*-acetylhexosamines and mono-sulfated *N*-acetylhexosamine-uronic acid disaccharides. Analysis of plasma and DBS on filter paper collected from MPS patients showed elevations of total mono-sulfated *N*-acetylhexosamines but less than that seen in urine. However, direct quantification of GAGs by mass spectrometry is complex because of their molecular heterogeneity, resulting in difficulty of application to mass screening and practical use for diagnosis of the patients.

The major GAGs that accumulate in MPS patients are copolymers that contain analogous repeating units (glucurono-, or idurono-sulfo-*N*-acetyl-glucosamine or galactosamine) [57]. These polymers are amenable to chemical and enzymatic degradation (methanolysis and hydrolysis) to produce simple molecules containing the repeating subunits. The sulfate groups are rapidly cleaved and the remaining acidic polysaccharides are hydrolyzed or methanolyzed at certain glycosidic linkages and dissociate to stable disaccharides as end products.

In 2007, Oguma and Tomatsu developed a highly sensitive, specific, accurate, and inexpensive strategy in which DS, HS, and KS disaccharides are produced from GAGs in blood and urine samples by hydrolysis and analyzed simultaneously by LC–MS/MS (Fig. 1) [56–58, 96–98]. Other groups have subsequently developed similar methods [99–100]. A significant advantage of this approach is that not only individual but multiple disaccharides are measured from a single sample, and that all types of MPS can be detected in a first-tier screening, with specific types confirmed in a second-tier screening. Blood, urine, or other biological samples are purified by filtration and GAGs digested with chondroitinase B, heparitinase, and keratanase II to yield disaccharides of DS, HS, and KS. After digestion, the samples are injected into the LC–MS/MS and results are compared with control samples (Fig. 2).

The LC–MS/MS method not only shows sensitivity and specificity for detecting all subtypes of MPS but also is able to monitor therapeutic efficacy in MPS patients and animal models [15,63,98–103]. This new method has an advantage of being both GAG-specific and quantitative.

In 2011, Auray-Blais et al. described that methanolysis can be used to prepare HS and DS for LC–MS/MS analysis from GAGs in urine of MPS patients [104,105]. Methanolysis has not yet been used to measure KS.

In 2012, Lawrence et al. showed that another new method with the enzyme digestion can detect DS and HS by analysis of non-reducing ends of urinary GAGs by LC–MS/MS. Currently, this method does not provide a measure of non-reducing ends for KS [106]. Overall, establishment of the method to measure the disaccharides rather than hetergenous oligosaccharides make it feasible to interpret individual GAG values, leading to rapid and accurate diagnosis, prognosis, and monitoring therapies for MPS.

3. Update of LC–MS/MS method with enzyme digestion

3.1. Equipment

At present, the following LC–MS/MS instruments have been confirmed to provide good resolution for disaccharide analysis by multiple laboratories; Alliance 2795XE HPLC system/Quattro micro tandem quadrupole (Waters Corp, Milford, MA, USA); Ultra performance liquid chromatography (UPLC) Acquity system/Xevo TQ-S (Waters Corp, Milford, MA, USA); HP1100 system (Agilent Technologies, Palo Alto, CA, USA)/API-4000 or API-5000 (AB Sciex, Foster City, CA, USA); Acquity HPLC system/Quattro Premier XE (Waters Corp, Milford, MA, USA); and 1260 infinity LC/6460 Triple Quad (Agilent Technologies, Palo Alto, CA, USA) [56–58,95–98,9–101,103–106, personal communication from Dr. K. Kida].

3.2. Standards

ΔDiHS-6S (HS); ΔDiHS-NS (HS); ΔDiHS-0S (HS); ΔDi-4S (DS); mono-sulfated KS — Galβ1-4GlcNAc(6S); di-sulfated KS — Gal(6S)β1-4GlcNAc(6S); and KS I (bovine cornea) digested with keratanase II to yield Galβ1-4GlcNAc(6S), Gal(6S)β1-4GlcNAc(6S), have all been used to produce standard curves for each specific GAG (Fig. 3). A common internal standard is chondrosine. The KS I standard is the most difficult to quantify. We assessed efficiency of KS I digestion by keratanase II using gel permeation chromatography. We found that 60% of KS I was digested with keratanase II and that the ratio of Gal(6S)β1-4GlcNAc(6S) to Galβ1-4GlcNAc(6S) was 42:58 (data not shown).

3.3. Disaccharide determination derived from GAGs

3.3.1. Recoveries

Extraction efficiencies of KS-derived and DS/HS-derived disaccharides from control samples are over 87% and almost 100%, respectively. These methods have been applied successfully to extract KS- and DS/HS-derived disaccharides from human serum [56,57].

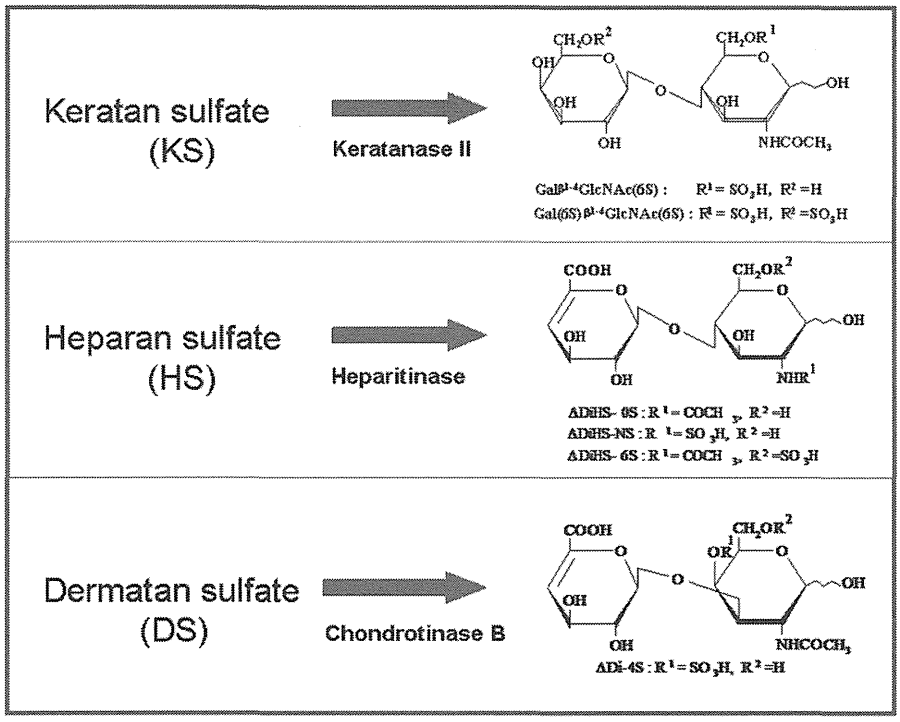

Fig. 1. Production of disaccharides digested by the enzymes.

3.3.2. Chromatography and selectivity

Chromatograms of extracts obtained from a control serum sample consist of Galβ1-4GlcNAc(6S), Gal(6S)β1-4GlcNAc(6S), ΔDiHS-0S, ΔDiHS-NS, and ΔDi-4S. All disaccharides are eluted in less than 5 min (see Figs. 3, 4) [56,57].

3.3.3. Calibration curves

Calibration parameters of disaccharides derived from DS, HS, and KS and in human serum were assessed. Calibration curves for Galβ1-4GlcNAc(6S), Gal(6S)β1-4GlcNAc(6S), ΔDiHS-0S, ΔDiHS-NS, and ΔDi-4S obtained on five separate days are linear over the concentration ranges of 0.14 to 7.1 μg/ml, 0.06 to 2.9 μg/ml, 10 to 1000 ng/ml, 5 to 500 ng/ml, and 10 to 1000 ng/ml, respectively. The correlation coefficients of determination (r) are not less than 0.99 [56,57].

3.3.4. Precision

The results of intra- and inter-assay precision for ΔDiHS-0S, ΔDiHS-NS, and ΔDi-4S in control serum are as follows. The disaccharide (ΔDi-4S) is detected by the same ions (m/z 462/97) as those of ΔDiHS-6S. Thus, the total concentration of disaccharides expressed as ΔDi-4S includes both ΔDi-4S and ΔDiHS-6S. The intra-assay precision values/coefficient of variation (CV) determined from analysis of ΔDiHS-0S, ΔDiHS-NS, and ΔDi-4S for control serum are less than 6.7, 7.9, and 15.8%, respectively. The inter-assay precision values/CVs for these disaccharides in control serum are less than 5.2, 6.8, and 14.8%, respectively. The intra-assay precision values/CVs for Galβ1-4GlcNAc(6S) and Gal(6S)β1-4GlcNAc(6S) in control serum were less than 8.2 and 5.3% and inter-assay precision values/CVs were less than 6.6 and 5.7%. These results demonstrate the reproducibility and accuracy of the method [56,57].

3.4. Analysis of plasma and serum samples in MPS patients

Each type of MPS has a different pattern of elevated GAG levels in serum or plasma. We described concentrations of DS-, HS-, and KS-derived disaccharides and their composition ratios in human control and MPS patients [56–58].

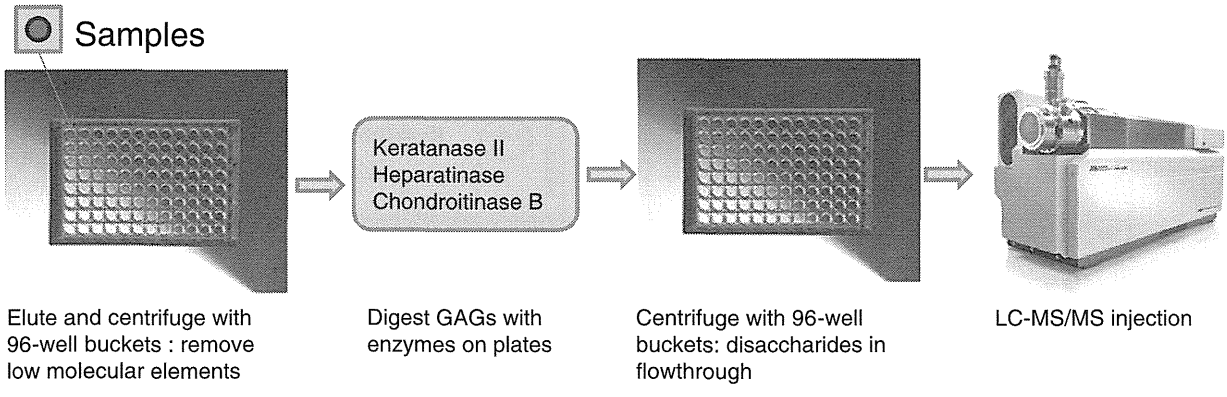

Fig. 2. Sample preparation and apparatus with automated procedure.

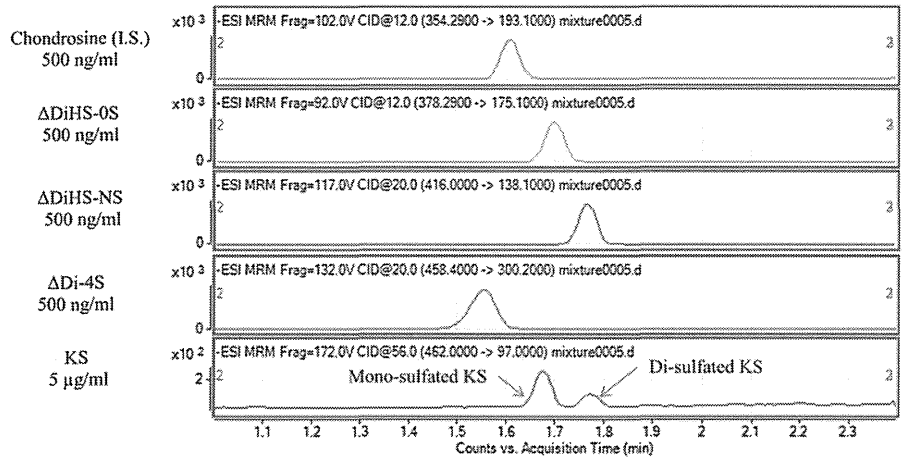

Fig. 3. Chromatograms for KS-I (bovine cornea), ΔDi-4S (DS), ΔDiHS-NS, ΔDiHS-0S, and chondrosine (IS) disaccharides by using Hypercarb (2.0 mm × 50 mm, 5 μm; Thermo Electron Corp.) with a solvent gradient of 0% to 100% 5 mM ammonium acetate (pH 10):acetonitrile. Polymer KS was separated with mono-sulfated KS [Galβ1-4GlcNAc(6S)] and di-sulfated KS [Gal(6S)β1-4GlcNAc(6S)] after digestion by keratanase II. Equipment: 6460 Triple Quad MS/MS with 1260 infinity LC (Agilent Technologies). IS: internal standard.

3.4.1. Diagnosed MPS patients

Plasma samples were digested by heparitinase and chondroitinase B to produce disaccharides of DS and HS. Digested samples were assayed by LC–MS/MS. For the DS and HS assay, 120 samples from patients (MPS I, 22; MPS II, 27; MPS IIIA, 5; MPS IIIB, 4; MPS IIIC, 2; MPS IVA, 42; MPS VI, 4; MPS VII, 6) (age; 0–66 years) and 112 control samples (age; 0–62 years) were analyzed. The results were as follows.

- All MPS I, II, IIIA, IIIB, IIIC, and VI patients had significant elevations of plasma DS + HS (ave. 3024; 2763; 2610; 2933; 1605; 2700 ng/ml, respectively; min. 829 ng/ml, max. 23,800 ng/ml), compared with controls (ave. 448 ng/ml, min. 107 ng/ml, max. 776 ng/ml, $p < 0.0001$) (Figs. 4, 5). Specificity and sensitivity are 100%, if the cut-off value is 800 ng/ml between control and MPS samples [58].
- All MPS VI patients have significant elevation of plasma DS (ave. 2225 ng/ml, min. 1100 ng/ml; max. 4400 ng/ml), compared with controls (ave. 253 ng/ml, min. <1 ng/ml; max. 610 ng/ml; $p < 0.0001$) [58].
- Forty-four blood specimens from MPS IVA patients (ages 2–65 years; mean 14.3 years) were analyzed to confirm that the KS concentration is a suitable marker for early diagnosis and longitudinal assessment of disease severity. Blood specimens were obtained from patients categorized phenotypically as severe ($n = 33$), and attenuated ($n = 11$). Plasma samples were digested by keratanase II to produce disaccharides of KS [95,96].

Digested samples were assayed by LC–MS/MS. Plasma KS levels varied with age and clinical severity. Plasma KS levels in healthy controls

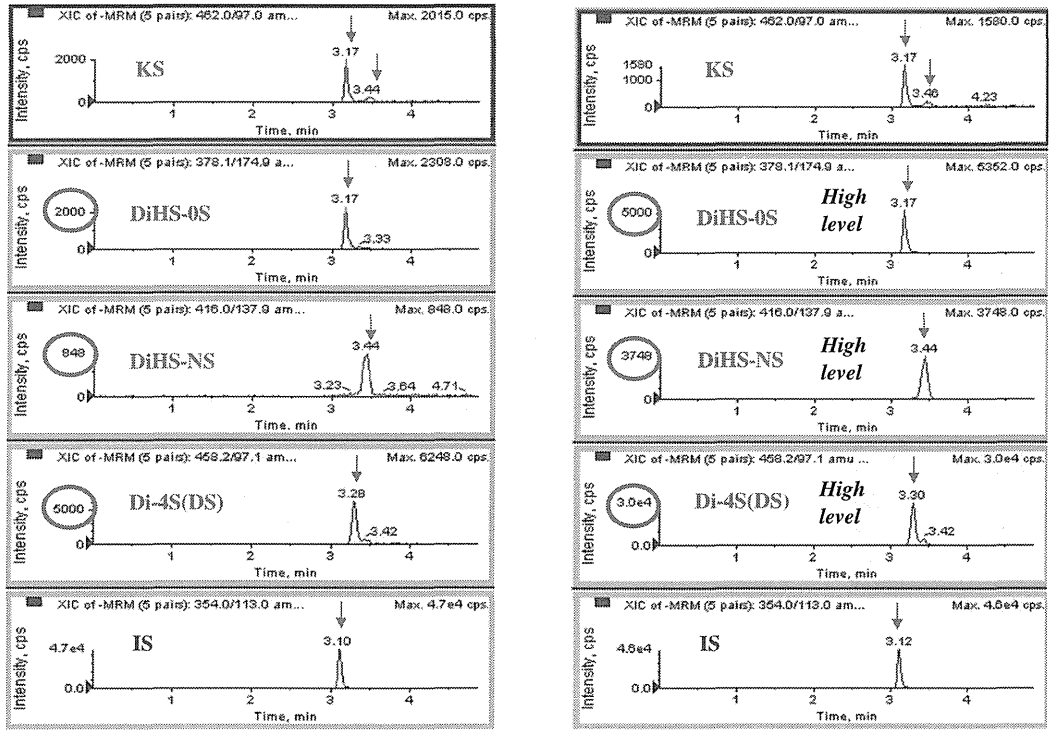

Fig. 4. Chromatograms of extracts from control (left) and MPS II (right) blood spots. Equipment; HP1100 system/API-4000. The arrows show the peaks of each disaccharide. KS has two peaks: mono-sulfated KS [Galβ1-4GlcNAc(6S)] (a major peak) and di-sulfated KS [Gal(6S)β1-4GlcNAc(6S)].

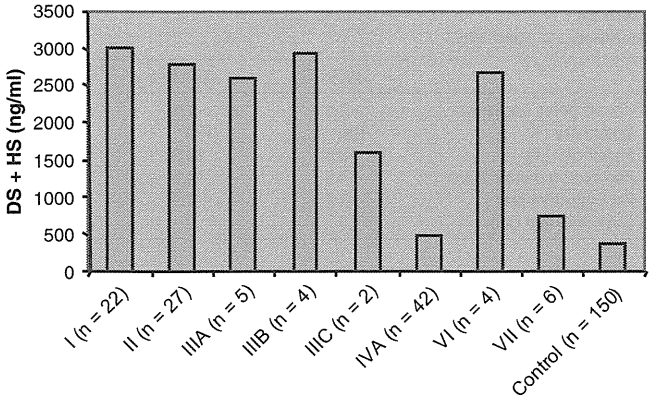

Fig. 5. Total DS and HS levels in blood of MPS patients. Equipment; HP1100 system/API-4000.

(n = 90) in 0–5 years showed 1.843 ± 0.0634 μg/ml while plasma KS levels in MPS IVA patients (n = 25) showed 7.445 ± 3.042 μg/ml ($p < 0.0001$). There was no overlap in blood KS value between the age-matched MPS IVA patients and healthy controls (see Fig. 6), although there was no case of newborn MPS IVA available. By contrast, the predictive value of KS in older patients was poor, with levels indistinguishable from controls (Fig. 6). This clearly demonstrates that test should be performed at an early stage.

Thus, we can not only screen for a group of MPS but also infer MPS subtypes from specific patterns of elevation of each GAG, leading to simplification of the second-tier enzyme assays designed as confirmatory diagnostic tests to identify the deficient enzyme. These findings suggest that measurement of DS, HS, and KS levels by LC–MS/MS can be applied to screening for MPS I, II, III, IV, VI, and VII patients.

3.4.2. Monitoring therapies

3.4.2.1. MPS VII mice treated by ERT. We treated MPS VII mice with 12 weekly infusions of human β-glucuronidase (GUS), modified GUS, or vehicle control, and monitored DS (ΔDi-4S) and HS (ΔDiHS-0S plus ΔDiHS-NS) levels.

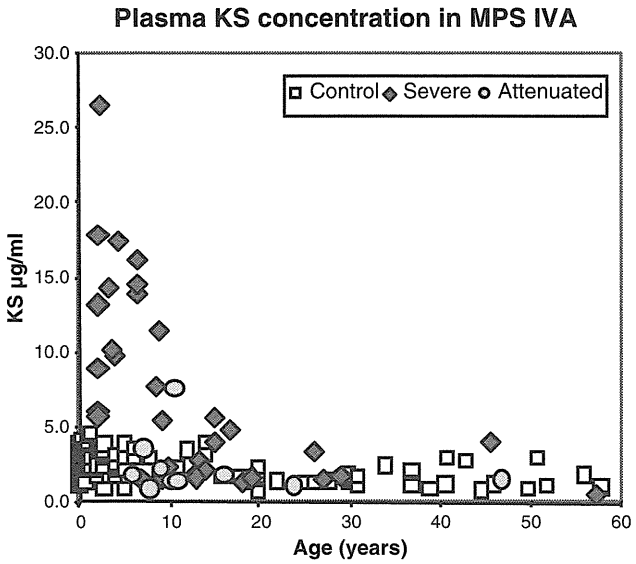

Fig. 6. Age-dependent KS in MPS IVA patients. White square; controls, red rhombus; MPS IVA patients with a severe form, green circle; MPS IVA patients with an attenuated form. Equipment; HP1100 system/API-4000.

Serum DS was elevated in untreated mutant mice over levels found in heterozygous control mice. Serum DS concentrations in untreated mice increased with age and reached over 7000 ng/ml by age 7 months. Serum HS concentrations in untreated mutant mice increased with age and reached around 4000 ng/ml by age 7 months. Serum HS in untreated mutant mice was significantly elevated at age 3 months compared with heterozygous control mice that had a relatively constant low level of HS over 7 months.

After 12 weekly infusions, all forms of GUS lowered serum DS and HS levels markedly. The concentration of serum DS was lower in mice treated with enzyme tagged with a short peptide consisting of acidic amino acids (D6- or D8-GUS) than the untagged enzyme (GUS). The same trend was seen for serum HS concentrations. The final serum HS in native GUS treated mice was higher than HS levels in tagged-GUS treated mice. Thus, this LC–MS/MS method shows efficacy of treatment with different enzyme formulations confirming the utility of this method for measuring biomarkers associated with MPS [63,107].

3.4.2.2. MPS IVA mouse treated by ERT. Mouse serum KS is not measurable by standard methods due to limited KS synthesis in rodents. The sensitivity of LC–MS/MS makes it feasible to assay serum KS in mice [15]. We treated MPS IVA mice with recombinant N-acetylgalactosamine-6-sulfate sulfatase (GALNS) and a sulfatase-modifier-factor 1 modified form of GALNS, for 12 weekly infusions. Serum KS levels were significantly reduced by 3 weeks compared with untreated mice and continued to decline over the 12 week duration of treatment. After 12 weeks of infusion, the average levels of serum KS were similar to those of normal mice [15].

3.5. Analysis of DBS samples in newborn controls and MPS patients

3.5.1. Newborn screening of MPS and its significance

NBS is recognized internationally as an essential, preventive public health program for early identification of disorders in newborns that can affect their long-term health. Early detection, diagnosis, and treatment of certain genetic, metabolic, or infectious congenital disorders can lead to significant reductions in disease severity, associated disabilities, and death. Currently, NBS represents the largest source of samples subjected to biochemical genetic testing worldwide. In the United States, the panel of NBS disorders varies from state to state, and decisions for adding or deleting tests involve many complex social, ethical, and political issues. Usually, disorders selected for NBS are tied to issues such as disorder prevalence, sensitivity, treatment availability, outcome, and overall cost effectiveness. Presently, NBS programs utilizing improvements in MS/MS screening procedures, screen for almost 50 disorders at birth and the number will continue to increase.

In the United States, NBS is performed for nearly 4.2 million neonates every year [108]. Almost 200 of these neonates are likely to be affected with MPS. Early detection of MPS would enable genetic counseling of the parents and early treatment. At present NBS for MPS I has been conducted by the enzyme assay method and three patients were found [9]; however, NBS for other types of MPS has not started yet. Thus, a presumptive diagnosis of most MPS patients is made much later when children present with clinical signs and symptoms. Establishing standard methodologies to screen MPS at an early clinical stage should improve the clinical course significantly. Early detection allows medical intervention, which may ultimately slow progression of the disease and reduce morbidity and mortality [109]. There are several important factors supporting a decision to include MPS into NBS programs:

- Number of patients: Incidence of MPS collectively is higher than 1 out of 25,000 births and annually nearly 200 newborns are expected to be diagnosed with MPS in the United States.
- Clinical course: The onset of severe forms of these diseases occurs prior to one year of age, while the diagnosis is typically delayed

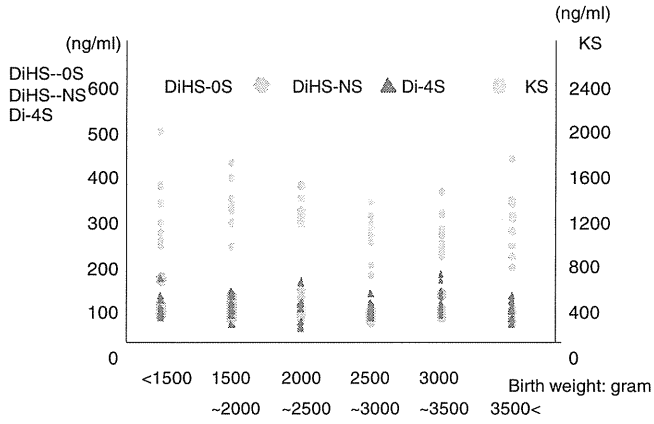

Fig. 7. Distribution of each GAG level in DBS of normal newborns by birth weight. Average of ΔDiHS-0S, ΔDiHS-NS, and ΔDi-4S was 347 ng/ml (range: 282–502), 85 ng/ml (range: 64–159), and 96 ng/ml (range: 57–163), respectively. The average of KS was 1185 ng/ml (range: 684–1511). Yellow: ΔDiHS-0S, green: ΔDiHS-NS, pink: ΔDi-4S, blue line: KS. Equipment; HP1100 system/API-4000.

until between two and four years of age for most types of MPS. Delay in diagnosis may lead to irreversible damage to bone and brain, resulting to early death.

- Availability of therapies: ERT, HSCT, and/or SRT treatments are available for several types of MPS. Clinical and experimental studies on MPS patients and animal models show that early diagnosis and early treatment provide better outcomes for these disorders.
- Natural history: The natural history of most types of MPS is under investigation and our understanding of the clinical features and their progression is evolving. Efficient and accurate NBS will prevent birth defects and will provide the affected infants a better quality of life.

Thus, we propose here a novel NBS system for MPS screened by LC–MS/MS.

To confirm effectiveness of simultaneous DS, HS, and KS assay by LC–MS/MS on DBS, we have analyzed DBS samples from newborn normal controls and newborns with MPS.

3.5.2. Normal healthy newborns

We measured ΔDiHS-0S, ΔDiHS-NS, ΔDi-4S, and KS extracted from DBS of healthy normal newborns. We classified DBS samples into 6 groups by birth weight (<1500 g, 1500–1999 g, 2000–2499 g, 2500–2999 g, 3000–3499 g, >3500 g). Each group was comprised of 10 samples. We did not observe any significant difference in overall GAG composition by birth weight (Fig. 7).

Table 2
HS and DS levels from dried blood spot in six MPS newborns and controls (ng/ml).

Case	ΔDiHS-0S	ΔDiHS-NS	ΔDi-4S	Total HS/DS
Case 1 (MPS I)	277	158	1090	1525
Case 2 (MPS I)	285	180	1200	1665
Case 3 (MPS I)	280	110	2266	2656
Case 4 (MPS I)	4503	6700	67,222	78,425
Case 5 (MPS VII)	408	406	3417	4231
Case 6 (MPS II)	240	137	836	1210
Control (n = 326)				
Mean ± SD	117 ± 23	67 ± 28	370 ± 109	553 ± 146

Table 3
Sensitivity and specificity.

	ΔDiHS-0S	ΔDiHS-NS	ΔDi-4S
Cut off point (ng/spot)	>2.5	>1.1	>8.0
Sensitivity (%)	100	100	100
Specificity (%)	98.5	98.5	99.7
Positive predictive value	54.5	54.5	85.7
False positive rate	1.5	1.5	0.3
False negative rate	0	0	0

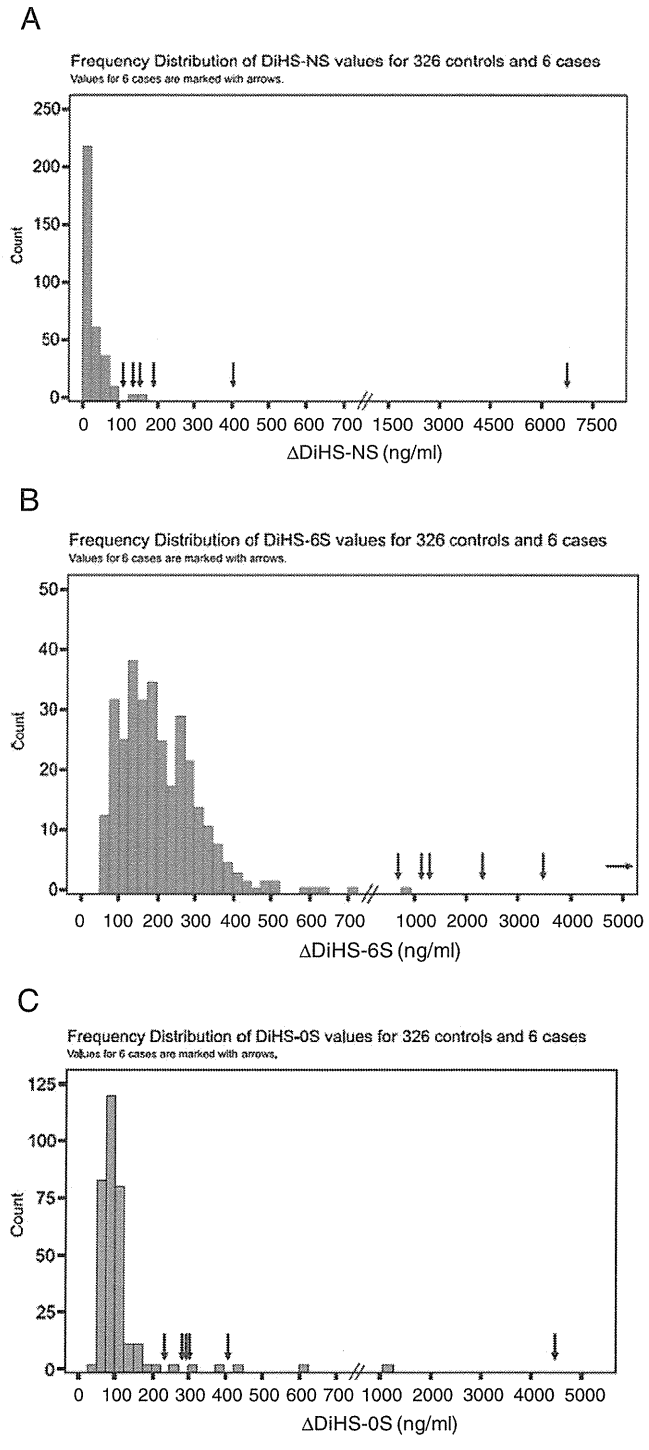

Fig. 8. Frequency distribution of A) ΔDiHS-NS, B) ΔDi-4S, and C) ΔDiHS-0S for DBS from 326 controls to 6 MPS cases. Values for 6 cases are marked with arrows. Bars represent controls with frequency. Equipment; HP1100 system/API-4000.

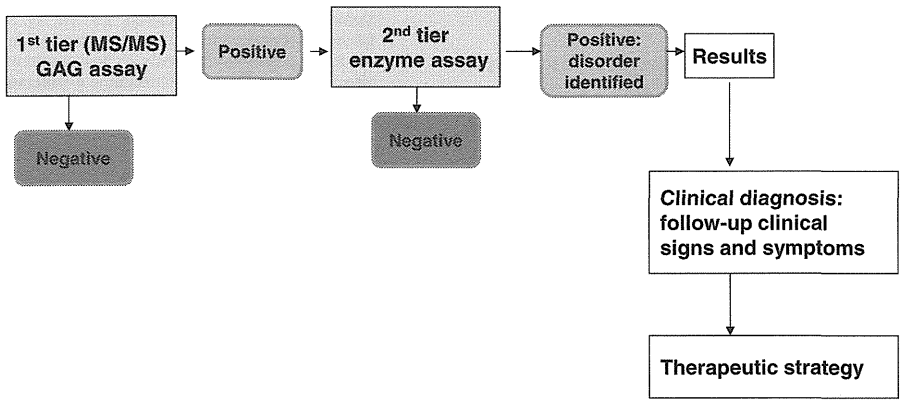

Fig. 9. Proposed two-tier strategy of newborn screening for mucopolysaccharidoses.

3.5.3. Newborn MPS

When the elevation of GAGs is first detectable in human MPS patients is unknown. To assess whether our LC–MS/MS method can distinguish MPS newborns from the normal control newborns, we compared DS and HS levels in DBS samples from six neonates that were subsequently determined to have MPS (four MPS I, one MPS II, and one MPS VII) and control newborns ($n = 326$) in a double blind manner. All six cases (Table 2) had marked elevations of DS and HS (above 1500 ng/ml) compared with the values of normal control newborns (mean, 553 ± 146 ng/ml). DS and HS levels in another DBS sample from a one year-old infant with MPS I (Case 3) remained high since this infant went untreated. This infant was a fraternal twin and DS and HS levels were clearly distinguishable between the unaffected and affected fraternal twin (800 ng/ml vs. 2660 ng/ml).

The overall performance metrics of ΔDiHS-0S (HS), ΔDiHS-NS (HS), and ΔDi-4S (DS) values were as follows using a given set of cut-off values (Table 3, Fig. 8): sensitivity, 100%; specificity, 98.5–99.4%; positive predictive value, 54.5–75%; false positive rate, 0.62–1.54%; and false negative rate, 0% in any of these biomarkers. In 2012, Paracchini et al. reported the results of NBS for CF by assaying the immunoreactive trypsinogen level with the cut off of >99th centile. The results showed that among a total of 717,172 newborns screened, 7354 newborns were found positive to NBS. After the second screening by sweat test, 7234 newborns (98.4%: false positive) were negative or not confirmed, while 120 newborns (1.6%) were confirmed as a patient with CF [61]. These results support our hypothesis that using the LC–MS/MS method to measure GAGs can be applied to NBS for MPS.

Subsequently, Ruijter et al. assayed DS and HS levels from newborn DBS of 11 MPS I, 1 MPS II, and 6 MPS III patients, with phenotypes ranging from severe to relatively attenuated forms. The levels of DS and HS derived disaccharides in these DBS were compared with levels in DBS of newborn MPS I and MPS III heterozygotes and controls. The levels of DS and HS derived disaccharides were clearly elevated in all newborn DBS of MPS I, II, and III patients when compared with controls. In contrast, DBS of MPS I and III heterozygotes showed similar disaccharide levels when compared with control DBS [100].

Potential advantages of this current method are: i) inclusion of all types of MPS for the first-tier screening; ii) prediction of MPS type with elevation of specific GAGs such as DS, HS, and KS or in combination and, iii) monitoring efficacy of therapies.

We are conducting a pilot study of NBS for MPS patients, supported by NIH (1R01HD065767-01), using this LC–MS/MS method. Fig. 9 describes the two-tier strategy of NBS for MPS. GAG assay is the first tier to define a high risk group of MPS. Subsequently, enzyme assays are performed on blood spots from this high risk group in a second tier to confirm diagnosis. Enzyme assays will be conducted by using synthetic substrates as described elsewhere [47–55].

3.6. Limitations of current LC–MS/MS method

A limitation of the current method is that there is a possibility that we may obtain false negative results in samples from patients with very mild phenotypes, although treatment of such patients in the newborn period would not typically be necessary. Another major limitation of this method could be the chromatographic time (≥4 min) of LC, still limited throughput for mass screening. We may need additional improvements in the method such as use of a RapidFire system (Agilent Technologies) for NBS in practice, in which every sample can be assayed within 10 s.

4. Conclusion

In conclusion, MS/MS methodology for the analysis of disaccharides of GAG has become popular and should be available in diagnostic and clinical settings soon. With increased demand for MS/MS assays and the wider availability of instrumentation, MS/MS methodologies are likely to have a large impact in screening, diagnosis, and monitoring of MPS in the future.

Acknowledgments

This work was supported by grants from the Austrian MPS Society, National MPS Society, International Morquio Organization (Carol Ann Foundation), and Delaware Bioscience Center for Advanced Technology. R.W.M. and S.T. are supported by National Institutes of Health grant 8P20 GM103464-08. S.T. and A.M are supported by National Institutes of Health grant 1R01HD065767-01. The content of the article has not been influenced by the sponsors. There is no conflict of interest with any co-author from the industry. Any industry has neither patent nor licensing agreement for the LC–MS/MS method on mucopolysaccharidoses described here. The patent right of the LC–MS/MS described here is solely owned by Saint Louis University to date. All enzymes are provided by Seikagaku Co. The corresponding author can provide the enzymes upon request. The instrument of 1260 infinity LC/6460 Triple Quad was kindly provided by Agilent Technologies.

References

[1] J.E. Wraith, The mucopolysaccharidoses: a clinical review and guide to management, Arch. Dis. Child. 72 (1995) 263–267.
[2] D.A. Applegarth, J.R. Toone, R.B. Lowry, Incidence of inborn errors of metabolism in British Columbia, 1969–1996, Pediatrics 105 (2000) e10.
[3] F. Baehner, C. Schmiedeskamp, F. Krummenauer, E. Miebach, M. Bajbouj, C. Whybra, A. Kohlschütter, C. Kampmann, M. Beck, Cumulative incidence rates of the mucopolysaccharidoses in Germany, J. Inherit. Metab. Dis. 28 (2005) 1011–1017.
[4] P.J. Meikle, J.J. Hopwood, A.E. Clague, W.F. Carey, Prevalence of lysosomal storage disorders, JAMA 281 (1999) 249–254.
[5] J. Nelson, Incidence of the mucopolysaccharidoses in Northern Ireland, Hum. Genet. 101 (1997) 355-258.
[6] J. Nelson, J. Crowhurst, B. Carey, L. Greed, Incidence of the mucopolysaccharidoses in Western Australia, Am. J. Med. Genet. A 123A (2003) 310–313.
[7] B.J. Poorthuis, R.A. Wevers, W.J. Kleijer, J.E. Groener, J.G. de Jong, S. van Weely, K.E. Niezen-Koning, O.P. van Diggelen, The frequency of lysosomal storage diseases in The Netherlands, Hum. Genet. 105 (1999) 151–156.
[8] H.Y. Lin, S.P. Lin, C.K. Chuang, D.M. Niu, M.R. Chen, F.J. Tsai, M.C. Chao, P.C. Chiu, S.J. Lin, L.P. Tsai, W.L. Hwu, J.L. Lin, Incidence of the mucopolysaccharidoses in Taiwan, 1984–2004, Am. J. Med. Genet. A 149A (2009) 960–964.
[9] C.R. Scott, S. Elliott, N. Buroker, L.I. Thomas, J. Keutzer, M. Glass, M.H. Gelb, F. Turecek, Identification of infants at risk for developing Fabry, Pompe, or mucopolysaccharidosis-I from newborn blood spots by tandem mass spectrometry. J. Pediatr. http://dx.doi.org/10.1016/j.jpeds.2013.01.031 [pii: S0022-3476(13)00065-6] [Epub ahead of print] [in press].
[10] A. Purushothaman, J. Fukuda, S. Mizumoto, G.B. ten Dam, T.H. van Kuppevelt, H. Kitagawa, T. Mikami, K. Sugahara, Functions of chondroitin sulfate/dermatan sulfate chains in brain development. Critical roles of E and iE disaccharide units recognized by a single chain antibody GD3G7, J. Biol. Chem. 282 (2007) 19442–19452.
[11] K. Sugahara, H. Kitagawa, Heparin and heparan sulfate biosynthesis, IUBMB Life 54 (2002) 163–175.
[12] J.L. Funderburgh, Keratan sulfate: structure, biosynthesis, and function, Glycobiology 10 (2000) 951–958.
[13] G. Schaison, P. Bordigoni, G. Leverger, Bone marrow transplantation for genetic and metabolic disorders, Nouv. Rev. Fr. Hematol. 31 (1989) 119–123.
[14] A. Vellodi, E. Young, A. Cooper, V. Lidchi, B. Winchester, J.E. Wraith, Long-term follow-up following bone marrow transplantation for Hunter disease, J. Inherit. Metab. Dis. 22 (1999) 638–648.
[15] S. Tomatsu, A.M. Montano, A. Ohashi, M.A. Gutierrez, H. Oikawa, T. Oguma, V.C. Dung, T. Nishioka, T. Orii, W.S. Sly, Enzyme replacement therapy in a murine model of Morquio A syndrome, Hum. Mol. Genet. 17 (2008) 815–824.
[16] J.H. Grubb, C. Vogler, W.S. Sly, New strategies for enzyme replacement therapy for lysosomal storage diseases, Rejuvenation Res. 13 (2010) 229–236.
[17] R.M. Shull, E.D. Kakkis, M.F. McEntee, S.A. Kania, A.J. Jonas, E.F. Neufeld, Enzyme replacement in a canine model of Hurler syndrome, Proc. Natl. Acad. Sci. U. S. A. 91 (1994) 12937–12941.
[18] A.C. Crawley, D.A. Brooks, V.J. Muller, B.A. Petersen, E.L. Isaac, J. Bielicki, B.M. King, C.D. Boulter, A.J. Moore, N.L. Fazzalari, D.S. Anson, S. Byers, J.J. Hopwood, Enzyme replacement therapy in a feline model of Maroteaux–Lamy syndrome, J. Clin. Invest. 97 (1996) 1864–1873.
[19] E. Downs-Kelly, M.Z. Jones, J. Alroy, K.T. Cavanagh, B. King, R.E. Lucas, J.C. Baker, S.A. Kraemer, J.J. Hopwood, Caprine mucopolysaccharidosis IIID: a preliminary trial of enzyme replacement therapy, J. Mol. Neurosci. 15 (2000) 251–262.
[20] E.D. Kakkis, J. Muenzer, G.E. Tiller, L. Waber, J. Belmont, M. Passage, B. Izykowski, J. Phillips, R. Doroshow, I. Walot, R. Hoft, E.F. Neufeld, Enzyme-replacement therapy in mucopolysaccharidosis I, N. Engl. J. Med. 344 (2001) 182–188.
[21] J. Muenzer, M. Beck, C.M. Eng, M.L. Escolar, R. Giugliani, N.H. Guffon, P. Harmatz, W. Kamin, C. Kampmann, S.T. Koseoglu, B. Link, R.A. Martin, D.W. Molter, M.V. Muñoz Rojas, J.W. Ogilvie, R. Parini, U. Ramaswami, M. Scarpa, I.V. Schwartz, R.E. Wood, E. Wraith, Multidisciplinary management of Hunter syndrome, Pediatrics 124 (2009) e1228–e1239.
[22] J. Muenzer, J.C. Lamsa, A. Garcia, J. Dacosta, J. Garcia, D.A. Treco, Enzyme replacement therapy in mucopolysaccharidosis type II (Hunter syndrome): a preliminary report, Acta Paediatr. Suppl. 91 (2002) 98–99.
[23] P. Harmatz, C.B. Whitley, L. Waber, R. Pais, R. Steiner, B. Plecko, P. Kaplan, J. Simon, E. Butensky, J.J. Hopwood, Enzyme replacement therapy in mucopolysaccharidosis VI (Maroteaux–Lamy syndrome), J. Pediatr. 144 (2004) 574–580.
[24] P. Harmatz, D. Ketteridge, R. Giugliani, N. Guffon, E.L. Teles, M.C. Miranda, Z.F. Yu, S.J. Swiedler, J.J. Hopwood, Direct comparison of measures of endurance, mobility, and joint function during enzyme-replacement therapy of mucopolysaccharidosis VI (Maroteaux–Lamy syndrome): results after 48 weeks in a phase 2 open-label clinical study of recombinant human N-acetylgalactosamine 4-sulfatase, Pediatrics 115 (2005) e681–e689.
[25] P. Harmatz, R. Giugliani, I. Schwartz, N. Guffon, E.L. Teles, M.C. Miranda, J.E. Wraith, M. Beck, L. Arash, M. Scarpa, Z.F. Yu, J. Wittes, K.I. Berger, M.S. Newman, A.M. Lowe, E. Kakkis, S.J. Swiedler, Phase 3 Study Group, Enzyme replacement therapy for mucopolysaccharidosis VI: a phase 3, randomized, double-blind, placebo-controlled, multinational study of recombinant human N-acetylgalactosamine 4-sulfatase (recombinant human arylsulfatase B or rhASB) and follow-on, open-label extension study, J. Pediatr. 148 (2006) 533–539.
[26] P. Harmatz, R. Giugliani, I.V. Schwartz, N. Guffon, E.L. Teles, M.C. Miranda, J.E. Wraith, M. Beck, L. Arash, M. Scarpa, D. Ketteridge, J.J. Hopwood, B. Plecko, R. Steiner, C.B. Whitley, P. Kaplan, Z.F. Yu, S.J. Swiedler, C. Decker, Long-term follow-up of endurance and safety outcomes during enzyme replacement therapy for mucopolysaccharidosis VI: final results of three clinical studies of recombinant human N-acetylgalactosamine 4-sulfatase, Mol. Genet. Metab. 94 (2008) 469–475.
[27] N.M. Ellinwood, C.H. Vite, M.E. Haskins, Gene therapy for lysosomal storage diseases: the lessons and promise of animal models, J. Gene Med. 6 (2004) 481–506.
[28] B.L. Hodges, S.H. Cheng, Cell and gene-based therapies for the lysosomal storage diseases, Curr. Gene Ther. 6 (2006) 227–241.
[29] J. Jakobkiewicz-Banecka, E. Piotrowska, M. Narajczyk, S. Baranska, G. Wegrzyn, Genistein-mediated inhibition of glycosaminoglycan synthesis, which corrects storage in cells of patients suffering from mucopolysaccharidoses, acts by influencing an epidermal growth factor-dependent pathway, J. Biomed. Sci. 16 (2009) 26.
[30] R.W. Farndale, D.J. Buttle, A.J. Barrett, Improved quantitation and discrimination of sulphated glycosaminoglycans by use of dimethylmethylene blue, Biochim. Biophys. Acta 883 (1986) 173–177.
[31] C.B. Whitley, J.R. Utz, Maroteaux–Lamy syndrome (mucopolysaccharidosis type VI): a single dose of galsulfase further reduces urine glycosaminoglycans after hematopoietic stem cell transplantation, Mol. Genet. Metab. 101 (2010) 346–348.
[32] C.B. Whitley, R.C. Spielmann, G. Herro, S.S. Teragawa, Urinary glycosaminoglycan excretion quantified by an automated semimicro method in specimens conveniently transported from around the globe, Mol. Genet. Metab. 75 (2002) 56–64.
[33] E.W. Gold, The quantitative spectrophotometric estimation of total sulfated glycosaminoglycan levels. Formation of soluble alcian blue complexes, Biochim. Biophys. Acta 673 (1981) 408–415.
[34] S. Bjornsson, Quantitation of proteoglycans as glycosaminoglycans in biological fluids using an alcian blue dot blot analysis, Anal. Biochem. 256 (1998) 229–237.
[35] M. Karlsson, I. Edfors-Lilja, S. Bjornsson, Binding and detection of glycosaminoglycans immobilized on membranes treated with cationic detergents, Anal. Biochem. 286 (2000) 51–58.
[36] M. Shinmei, S. Miyauchi, A. Machida, K. Miyazaki, Quantitation of chondroitin 4-sulfate and chondroitin 6-sulfate in pathologic joint fluid, Arthritis Rheum. 35 (1992) 1304–1308.
[37] K. Yoshida, S. Miyauchi, H. Kikuchi, A. Tawada, K. Tokuyasu, Analysis of unsaturated disaccharides from glycosaminoglycuronan by high-performance liquid chromatography, Anal. Biochem. 177 (1989) 327–332.
[38] H. Toyoda, Y. Demachi, S. Komoriya, N. Furuya, T. Toida, T. Imanari, Characterization and determination of human urinary keratan sulfate, Chem. Pharm. Bull. (Tokyo) 46 (1998) 97–101.
[39] A. Kinoshita, K. Sugahara, Microanalysis of glycosaminoglycan-derived oligosaccharides labeled with a fluorophore 2-aminobenzamide by high-performance liquid chromatography: application to disaccharide composition analysis and exosequencing of oligosaccharides, Anal. Biochem. 269 (1999) 367–378.
[40] H. Yamada, S. Miyauchi, M. Morita, Y. Yoshida, Y. Yoshihara, T. Kikuchi, O. Washimi, Y. Washimi, N. Terada, T. Seki, K. Fujikawa, Content and sulfation pattern of keratan sulfate in hip osteoarthritis using high performance liquid chromatography, J. Rheumatol. 27 (2000) 1721–1724.
[41] S. Tomatsu, K. Okamura, T. Taketani, K.O. Orii, T. Nishioka, M.A. Gutierrez, S. Velez-Castrillon, A.A. Fachel, J.H. Grubb, A. Cooper, M. Thornley, E. Wraith, L.A. Barrera, R. Giugliani, I.V. Schwartz, G.S. Frenking, M. Beck, S.G. Kircher, E. Paschke, S. Yamaguchi, K. Ullrich, K. Isogai, Y. Suzuki, T. Orii, N. Kondo, M. Creer, A. Noguchi, Development and testing of new screening method for keratan sulfate in mucopolysaccharidosis IVA, Pediatr. Res. 55 (2004) 592–597.
[42] S. Tomatsu, K. Okamura, H. Maeda, T. Taketani, S.V. Castrillon, M.A. Gutierrez, T. Nishioka, A.A. Fachel, K.O. Orii, J.H. Grubb, A. Cooper, M. Thornley, E. Wraith, L.A. Barrera, L.S. Laybauer, R. Giugliani, I.V. Schwartz, G.S. Frenking, M. Beck, S.G. Kircher, E. Paschke, S. Yamaguchi, K. Ullrich, M. Haskins, K. Isogai, Y. Suzuki, T. Orii, N. Kondo, M. Creer, T. Okuyama, A. Tanaka, A. Noguchi, Keratan sulphate levels in mucopolysaccharidoses and mucolipidoses, J. Inherit. Metab. Dis. 28 (2005) 187–202.
[43] S. Tomatsu, M.A. Gutierrez, T. Ishimaru, O.M. Peña, A.M. Montaño, H. Maeda, S. Velez-Castrillon, T. Nishioka, A.A. Fachel, A. Cooper, M. Thornley, E. Wraith, L.A. Barrera, L.S. Laybauer, R. Giugliani, I.V. Schwartz, G.S. Frenking, M. Beck, S.G. Kircher, E. Paschke, S. Yamaguchi, K. Ullrich, K. Isogai, Y. Suzuki, T. Orii, A. Noguchi, Heparan sulfate levels in mucopolysaccharidoses and mucolipidoses, J. Inherit. Metab. Dis. 28 (2005) 743–757.
[44] D. Matern, Newborn screening for lysosomal storage disorders, Acta Paediatr. Suppl. 97 (2008) 33–37.
[45] E. Parkinson-Lawrence, M. Fuller, J.J. Hopwood, P.J. Meikle, D.A. Brooks, Immunochemistry of lysosomal storage disorders, Clin. Chem. 52 (2006) 1660–1668.
[46] M.A. Tan, C.J. Dean, J.J. Hopwood, P.J. Meikle, Diagnosis of metachromatic leukodystrophy by immune quantification of arylsulphatase A protein and activity in dried blood spots, Clin. Chem. 54 (2008) 1925–1927.
[47] D. Wang, B. Eadala, M. Sadilek, N.A. Chamoles, F. Turecek, C.R. Scott, M.H. Gelb, Tandem mass spectrometric analysis of dried blood spots for screening of mucopolysaccharidosis I in newborns, Clin. Chem. 51 (2005) 898–900.
[48] M.H. Gelb, F. Turecek, C.R. Scott, N.A. Chamoles, Direct multiplex assay of enzymes in dried blood spots by tandem mass spectrometry for the newborn screening of lysosomal storage disorders, J. Inherit. Metab. Dis. 29 (2006) 397–404.
[49] G. Civallero, K. Michelin, J. de Mari, M. Viapiana, M. Burin, J.C. Coelho, R. Giugliani, Twelve different enzyme assays on dried-blood filter paper samples for detection of patients with selected inherited lysosomal storage diseases, Clin. Chim. Acta 372 (2006) 98–102.